# Chemical Synthesis at Surfaces with an Atomic Precision: Taming Complexity and Perfection

Can Wang,[a] Lifeng Chi,[b] Artur Ciesielski*[a] and Paolo Samorì*[a]

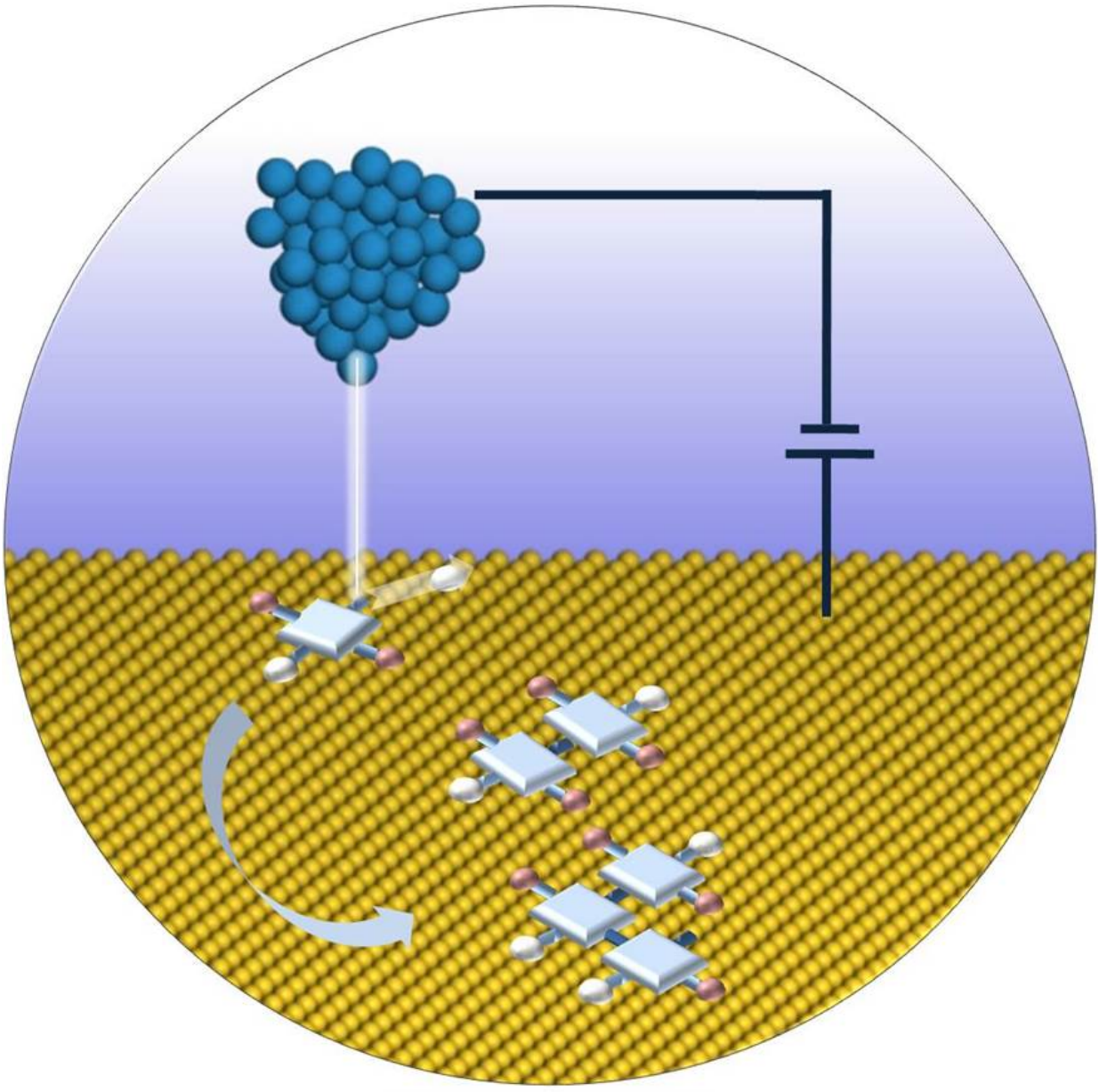

**Abstract:** Scanning probe microscopies (SPM) are powerful tools to study structure and dynamics of molecules at surfaces and interfaces as well as to precisely manipulate atoms and molecules by applying external force, by inelastic electron tunneling, or by means of an electric field. The rapid development of these SPM manipulation modes made it possible to achieve a fine control over fundamental processes in physics of interfaces and on chemical reactivity, such as adsorption, diffusion, bond formation and bond dissociation with a precision at the single atom/molecule level. Their controlled use for the fabrication of atomic-scale structures and synthesis of new – eventually uncommon - molecules with programmed properties are reviewed. Opportunity and challenges towards the development of complex chemical systems are discussed, by analysing potential future impacts in nanoscience and nanotech industry.

## 1. Introduction

The formation of a chemical bond represents the most fundamental process in chemistry which must be controlled with an atomic precision, towards the emergence of chemical complexity. Although by mimicking nature scientists were able to design and synthesize sophisticated artificial machines and devices, the level of structural and functional complexity which has been attained to date is very far from that of biochemical systems. From the first synthesis of Urea[1] and Vitamin $B_{12}$[2] to the successful fabrication of functional composite materials,[3] scientists have focussed their efforts towards gaining a deeper understanding of natural systems and processes thereof. However, the lack of powerful characterization tools assisting chemists in this path towards increasing complexity, by offering atomic mapping in the direct space, has hindered the in-depth understanding for several decades.[4]

The invention of Scanning Tunneling Microscopy (STM) by Binnig and Rohrer in the early '80s[5] has made it possible to image surfaces and interfaces with an atomic resolution in the real, i.e. direct, space. The working principle of STM is the tunneling of electrons between a sharpened metal probe (tip) and a conducting surface, when they are brought in close proximity. The highest tunability of the operating mode which is attained by modulating the tunneling parameters such as the bias voltage and the tunneling current makes it possible to work either in a non-invasive mode, enabling the mapping of the structure and dynamics of surfaces and interfaces with an atomic precision, or in more invasive regimes to controllably manipulate atoms and molecules.[6] In fact, upon applying a bias voltage between the tip and the sample surface, electrons tunneling or electric field emitted electrons can be exploited to trigger reactions, as they act as ultrasmall electron beam welder for breaking or creating chemical bonds. In STM imaging of an atom or molecule, the output tunneling current is roughly proportional to its local density of states (LDOS); as a result, the contrast in the so-called constant height mode appears brighter in electron-rich areas of the surface under investigation. The exponential dependence of the magnitude of the tunneling current on the separation distance between the tip and the conducting substrate surface makes it possible to position the tip accurately at a chosen distance above the surface with a sub-ångström precision.

When the first stable low-temperature STM was built at IBM Almaden Research Center in the late '80s, [7] scientists began extending the *human touch* to the atomic realm, by using the STM tip as manipulating tool. Tungsten tip prepared by electrochemical etching, having a conical shape with an atomic apex, was indeed first exploited for atomic manipulation. Since the first STM controlled atom-by-atom positioning,[8] a great deal of effort has been devoted towards the manipulation of individual atoms and molecules with atomic-scale precision.[9] The adjustment of the tip position may be employed for tuning the magnitude and nature of the tip-substrate interaction. By lowering the tip close to the surface one can obtain an overlap between the wave function of the atoms on the underlying surface and the outermost tip atoms, yielding repulsive forces that can be used to manipulate the adsorbate by pushing it across the surface. Eigler and Schweizer first showed that it is possible to slide atoms on Ni(111) surface, thereby writing the "IBM" logo by assembling Xe atoms, as displayed in Fig. 1b.[8] Towards this end, the following procedure (Fig. 1a) has been employed: *i*) the STM tip was approached toward an Xe atom physisorbed on a surface to increase the tip-atom interaction force; *ii*) the lateral displacement of the tip made it possible to re-locate the Xe atom along a desired path until it reached a predetermined position; *iii*) the tip was retracted to the initial imaging height while the Xe atom was left behind on the Ni(111) surface. This pioneering atom manipulation experiment has been followed by a multitude of works, e.g. rearranging Pt adatoms on Pt(111),[10a] building a triangular artificial structure consisting of 52 Ag adatoms on Ag(111) surface.[10b] Crommie, Lutz and Eigler first moved 48 Fe adatoms on Cu (111) surface to form a quantum corral with a radius of 7.13 nm.[11] The surface state electrons on Cu(111) were able to be confined in this closed circle structure defined by barriers built from Fe adatoms. Spatial image of the eigenstates of a quantum corral showed standing waves of concentric rings, which derived from the scattering of surface state electrons by Fe adatoms. Further research demonstrated that single molecules can also be moved by the STM tip, e.g. CO molecules on Pt(111).[10] All these atom manipulation have been rigorously performed in ultra-high vacuum (UHV) environment and at a temperature of a few degrees kelvin, in order to avoid atom diffusion occurring at room temperature. During the manipulation process the interaction between the atomically sharpened STM tip and either small (e.g. di- or tri-atomic) molecules or larger polyatomic molecules is rather different. This is because the size of the tip apex, which is

[a] Dr. C. Wang, Dr. A. Ciesielski and Prof. P. Samorì
Université de Strasbourg, CNRS, ISIS,
8 alleé Gaspard Monge, 67000 Strasbourg, France
E-mail: ciesielski@unistra.fr, samori@unistra.fr
[b] Prof. L.F. Chi
Institute of Functional Nano & Soft Materials (FUNSOM), Jiangsu Key Laboratory for Carbon Based Functional Materials & Devices,
Soochow University , Suzhou 215123, PRA

formed mostly by a single atom, can only strongly interact with 1-3 atoms of the surface which represent a small portion of a large molecule, e.g. C60 molecules on Cu(111)[12], Cu-tetra-(3,5-di-tertiary-butyl-phenyl)-porphyrin (Cu-TBPP) molecules on Cu(100)[13]. As the sliding resistance of an adsorbate (atom or molecule) mostly depends on its diffusion barrier with the underlying substrate, a larger tip-adsorbate interaction shall be employed by lowering the tip position, i.e. approaching it closer to the surface, in order to manipulate the strength of interactions between adsorbate and surface, like Pb atom and CO molecule on Cu(211).[14] Noteworthy, in such lateral process, the manipulated molecule remains adsorbed on the substrate surface.

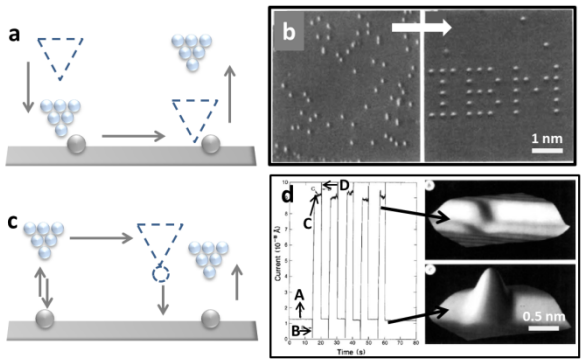


**Figure 1.** a) Schematic illustration of the lateral sliding process of an atom across a surface; b) "IBM" logo built by Xe atoms on Ni(111) surface. Reproduced from Ref.[8] with the permissions of the American Association for the Advancement of Science; c) Schematic illustration of the atomic transfer between surface and tip. d) The reversible transfer of Xe atom between the STM tip and Ni(111) surface. Low-conductance state with Xe atom on the surface (A). Current spike by applying -0.8 V pulse leading to the transfer of Xe atom to tip (B). High-conductance state with Xe atom on the tip (C). Applying 0.8 V pulse causing Xe atom to go back to the surface, regained state A (D), Reproduced from Ref.[15] with the permissions of the American Association for the Advancement of Science.

Alongside its use to generate lateral displacements of ad-atoms or ad-molecules, the STM tip can be employed to accomplish vertical manipulations, in which an atom or a molecule can be transferred from the surface to the STM tip and *vice versa*, as portrayed in Fig. 1c. To this end, external energy has to be delivered to overcome the energy barrier and allow the adsorbate transfer from the surface to the tip. Noteworthy, this energy barrier depends on the tip-surface separation distance, and it approaches zero when the tip is close enough to the adsorbate. In vertical manipulation processes, the major contribution to this external energy applied to the adsorbate comes from the electrons tunneling. Such a vertical manipulation process was first introduced to reversibly transfer Xe atom between a polycrystalline tungsten tip and a Ni(110) surface.[15] By applying a positive or negative voltage pulse of 0.8 V between the tip and the surface, the location of the Xe atom could be adjusted, i.e. the Xe atom could be picked up by the tip or deposited on the Ni(110) surface at desired position. The position of the Xe atom was identified by measuring the tunneling current during this transfer operation. As shown in Fig. 1d, the output tunneling current displayed two values depending on whether the Xe atom was bound to the surface (low) or to the tip (high). In a similar approach, the desorption of H atoms from Si(100)-2×1 surface was accomplished by applying a bias voltage greater than 2 V.[16] The same group subsequently reported an isotope effect on atom desorption, where the desorption yield of H atoms was about two orders of magnitude larger than that of D atoms.[17] More tightly bonded CO molecule on Cu(111) could be transferred to the tip by applying a high bias voltage larger than 3 V.[18] Further research on the mechanism of the process indicated that the manipulation of CO by a STM tip originated from a single electron excitation process of the CO-2π* orbital.[19] Noteworthy, the dependence of the CO transfer rate on the current at a fixed bias was found to be linear. The highest control over this process made it possible to realize the world's smallest stop-motion film - "a boy and his atom".

Lateral sliding and vertical transfer manipulations represent the most prototypical artificially controlled displacement of atoms and molecules. Such processes are of paramount importance for catalyzed reactions occurring at surfaces and interfaces,[20] to enable reactants (atoms or molecular fragments) to get in physical proximity, further leading to the formation of new chemical species *via* bond formation. In classical chemistry, reactants diffusion naturally occurs through thermally activated processes. The surface-potential energy landscapes greatly influence the direction and path of the thermodynamically governed diffusion processes. However, tip-induced diffusion can guide the reactants to a target position through a desired path. Moreover, large molecules may change their internal conformation along with the change of position.[21] For example, Moresco and co-workers showed that by using lateral manipulation on Cu-TBPP molecule on Cu(211), the conformation of a single tert-butyl-phenyl-group with respect to the substrate surface could be modified.[21b]

A classical chemical reaction can be divided into several steps, with each step being characterized by the dissociation and the formation of chemical bonds. The ability to describe the process during each individual bond formation could provide an indication about how well we understand reactions in nature. Supersonic molecular beam,[22] and femtosecond laser[23] have become important methods to study the molecular reaction involving isolated molecules and made it possible to probe the dynamics and reaction time scales of individual bond formation. Yet, STM offered a novel visual approach to monitor the chemical reaction process. Combined with the complementary tunneling spectroscopy measurements,[24] the chemical, physical, electronic, and mechanical properties of a single molecule can be unravelled at each reaction step with atomic-level resolution. The tip-induced reaction experiments are typically studied at low-temperature and under UHV to avoid occurrence of thermal-activated processes. Owing to these advantages, atom manipulation by STM has become an intriguing sub-field of nanochemistry.

In this manuscript we review the process of molecular synthesis occurring *via* controlled atom manipulations as unveiled by scanning tunneling microscopy imaging. In section 2,

we focus on controlled bond dissociation. Section 3 discusses the tip-induced bond formation, as well as classic examples of thermally activated bond formation. In section 4, we describe chemical and physical processes taking place in the junction between the STM tip and conductive substrates.

## 2. Unimolecular reactions: chemical bond dissociation

The deposition of a molecule onto a solid surface results in the weakening of the intramolecular bonds, because of the competition with molecule-surface interactions. In some cases, the intramolecular bonds can even dissociate upon the molecular adsorption onto catalytically active surfaces, as evidenced by the dehydrogenation of boric acid group upon physisorption on Ag (111).[25] Bond dissociation to generate reactive precursors is a key step in surface catalyzed molecular synthesis, to enable new chemical bonds formation, yielding novel chemical species. Since molecules tend to be mobile on surfaces, the tip-induced bond-breaking processes are favoured at low temperatures, by minimizing thermal diffusion. To dissociate a molecule by means of the STM tip, the energy required to break the chemical bond needs to be introduced in the system. Towards this end, two main approaches can be exploited as discussed below in this section.

### 2.1. Electric field

When the STM tip is brought into close proximity with the surface, by applying a bias voltage, an electric field as high as ca. 100 V $cm^{-1}$ can be generated [26], thus having a magnitude sufficient to break inter-atomic covalent bonds. As illustrated in the scheme in Fig. 2a, the effective area of the electric field is larger than atomic dimension. As the intensity of the electric field displays circular gradient distributed on the surface, the threshold of the field required for chemical bond dissociation imposes a strong space dependence by limiting the reaction in a certain area, i.e. where the centre of the field is located. Since the strength of this electric field is highest at apex of the tip, it is possible to manipulate surfaces with a true atomic resolution. By exploiting this method, Swartzentruber *et al.* reported for the first time the generation of an atomic-scale "bit" by moving single Ge atom from Ge(111)-2×8 surface.[27] The atomically resolved imaging of the defect-free region (Fig. 2b left) chosen for the atom manipulation was obtained under the scanning bias voltage of -1 V. By increasing the tip-to-surface bias to -4 V, successful dissociation of Ge-Ge covalent bonds was triggered and followed by a rapid withdrawal of the tip from the surface by 1 Å, and reduction of bias voltage to 1V in order to return to an imaging mode. The creation of a new protrusion in a previously pristine region of Ge(111) surface demonstrated the smallest spatial rearrangement of Ge atoms.

The mechanism of atom dissociation from the crystal surface was discussed by Lyo and Avouris through Si-Si bond breaking on Si(111)-7×7 surface.[28] By combining the effects of the strong tip-surface electric field with chemical tip-sample interactions, they reproducibly transferred Si atoms (Fig. 2c) or Si clusters containing tens of atoms from the surface to the tip and vice versa. The magnitude of tip-surface interactions and the number of transferred atoms were precisely controlled by applying voltage pulses at different tip-surface distances. It was found that the threshold field in this tip manipulation process (1 $VÅ^{-1}$) was significantly lower than that observed in field ion microscope studies (3.0-3.8 $VÅ^{-1}$).

On-surface Si atom manipulation was further studied by Aono *et al.*, by investigating the chemical reactivity of center adatom sites in Si(111)-7×7 lattices.[29] The single Si atom extraction process allowed the quantification of the excitation probabilities of the center and corner adatoms. The experimental results demonstrated that Si adatoms at the center of the 7×7 unit cell were more frequently removed than those near the corner holes. Such phenomenon was ascribed to the 0.1 eV binding energy difference between center and corner adatoms. Similar conclusions have been drawn by Dujardin *et al.*, who studied the Ge manipulation on Ge(111) surface.[30] Under electric field, an individual Ge atom was extracted in a controlled manner from a predefined site of the reconstructed Ge(111) surface. The statistical analysis of the adatom configurations observed around the vacancy made it possible to determine the free energy difference (0.15 eV) between the stable and metastable sites. Furthermore, Himpsel *et al.* manipulated Si atoms on Si(111)-5×2-Au surface at room temperature to propose a high storage density memory device.[31]

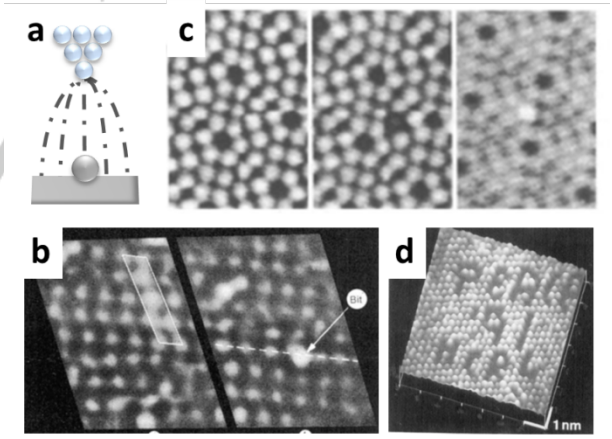


**Figure 2.** a) Schematic illustration of electric field created between STM tip and the surface. b) The c-(2×8) reconstructed Ge(111) surface before and after tip-induced manipulation. Left: a single unit cell of the c-(2×8) reconstruction highlighted in white. Right: the displayed region slightly translated due to the thermal drift, and the new bright spot near labeled with arrow was the impressed bit. Reproduced from Ref.[27] with the permissions of the American Association for the Advancement of Science. c) The process of removal of a single Si atom from Si(111)-7×7 surface. From left to right the images were taken before and after the voltage pules were applied, and after the re-deposition of the Si atom back to the surface. Reproduced from Ref.[28] with the permissions of The American Association for the Advancement of Science. d) Removing sulfur atoms from layer compound $MoS_2$ to form "PEACR `91 HCRL" characters. Reproduced from Ref.[32] with the permissions of the Elsevier B.V.

The single sulfur atom dissociation from layered semiconducting molybdenum (IV) disulfide ($MoS_2$) surface by tip-induced Mo-S bond tearing was successfully demonstrated by Hasegawa and co-workers.[32] The probe tip was moved to produce nanostructures by applying -5.5 V voltage, as displayed in Fig. 2d. Noteworthy, it was shown that related materials, e.g. tungsten (IV) diselenide ($WSe_2$) could also be manipulated, and nanosized hill structures can be reversibly produced and erased.[33] It should be noted that this experiment was carried out under ambient conditions, and therefore these results are certainly worthwhile to be pursued further for building-up stable artificial structures in air.

Noteworthy, by maintaining the tip at a higher distance from the surface, the electric field expands over a larger surface area, leading to multiple molecules reacting from only one voltage pulse. As proof-of-concept, this approach was employed to trigger reversibly the *trans*-to-*cis* isomerization of azobenzene derivatives on Au(111).[34] The groups of Grill and Hecht revealed the occurrence of spatial selectivity during the collective isomerization within the same molecular islands.[35] The switching possibility of individual 4-methoxy-3,30,5,50-tetra -tertbutylazobenzene (M-TBA) molecule on Au(111) was found to be strongly dependent on the arrangement of surrounding molecules. Only certain *trans*-M-TBA molecules in a specific self-assembled domain could be switched upon applying a voltage pulse, and therefore a distinct periodic pattern of *cis* isomers was generated.

Another effect is the controlled collection and repulsion of Cs atoms on GaAs(110) surface.[36] By applying an positive voltage pulse, Cs atoms were induced to diffuse into the region underneath the tip, thereby creating nanowire structures with lengths up to a few tens of nanometers.

### 2.2. Electron injection

Based on the electron energy, the bond dissociation induced by electron injection can be divided into field emission and inelastic tunneling approaches.[37] In the field emission process, the STM tip acts as an electron emission gun. High-energy electrons (roughly above 3 eV) can be emitted when the bias voltage exceeds the work function of the tip, e.g. 4.5 V for tungsten.

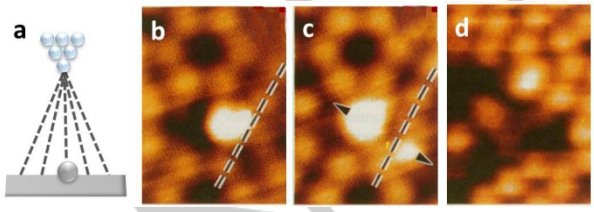


**Figure 3.** a) Schematic illustration of field-emitted electrons. b-d) An isolated $B_{10}H_{14}$ molecule (large white spot) adsorbed on Si(111)-7×7 (b). The result of electron bombardment at a bias voltage of + 8V, and an additional fragment dissociated from the $B_{10}H_{14}$ molecule appeared (c). Continuous scanning, the large molecule dissociated to yield a number of small fragments (d). Reproduced from Ref. [38a] with the permissions of the American Association for the Advancement of Science.

The tip-surface separation distance needs to be increased to above 10 Å to avoid an exceedingly large tunneling current. Therefore, tip manipulations with field emission electrons are impossible to be confined to the atomic size, since a significantly large areas (ca. 100 $Å^2$) are typically affected (Fig. 3a).

In the early 1990s, Avouris's group demonstrated the dissociation of $B_{10}H_{14}$ and $O_2$ molecules from Si(111)-7×7.[38] High bias voltages were used to rule out mechanical interactions between the tip and surface, suggesting that the observed dissociation processes were a direct consequence of electrons incident on the adsorbed molecules. The dissociation of an isolated $B_{10}H_{14}$[38a] at room temperature required a bias voltage at least of +4.0 V, and a high dissociation probability up to 80% was evidenced by increasing the bias to +8.0 V. The STM images of sequential dissociations are portrayed in Fig. 3b. A parent molecule was first dissociated with one emission electron and the fragments continued to be further dissociated over the scanning duration.

The tip-emitted electrons were also used to demonstrate the initial stages of Si(111)-7×7 oxidation by locally inducing $O_2$ desorption and dissociation (bias voltage of +7.0 V).[38b] The $O_2$ molecules were found as two chemisorbed species on silica - one bonded to an already oxidized Si adatom, and the other bonded to a second-layer rest Si atom.

Quantum tunneling effects can be generated when operating with a close tip-surface distance (< 1 nm). By applying low bias voltage, STM tip injects lower-energy electrons into the molecule *via* an adsorbate-induced resonance state, as depicted in Fig. 4a. The energy from the tunneling electrons transferred to the target molecule can lead to the dissociation if it exceeds the bond breaking energy barrier. In this inelastic tunneling dissociation process, the tunneling electrons confine the initial excitation to an atomic dimension below 1 Å, thus making it possible the selective targeting of a single bond. Furthermore, the amount of the tunneling electrons can be varied to control the reaction rate and pathway, thereby achieving localized and controllable bond dissociations. The reversible displacement of Si adatoms on Si(111)-7×7 surface at 52 K was reported by Ho and co-workers.[39] A bias voltage of 3 V was applied above a Si adatom to break Si-Si bond, as depicted in Fig. 4b-d. The displaced atoms were metastable and would be corrected (back to initial position) by tunneling or field-emitted electrons and by annealing above 155 K. Remarkably, such Si adatom displacement was found to be site-specific with a greater probability of the centre Si adatoms to be affected. Moreover, this displacement rate was found to linearly depend on the tunneling current, demonstrating that the dissociation of one Si adatom from surface can be stimulated by the tunneling of one electron from the STM tip.

The dissociation of diatomic molecules on surfaces is one of the simplest surface chemical reactions. Ho *et al* studied the mechanism of single $O_2$ molecule dissociation.[40] Towards this end, a single $O_2$ molecule has been imaged on the Pt(111) surface at low temperature (50 K) and dissociated using tunneling electrons from the precisely positioned STM tip, without affecting neighbouring molecules. Because this experiment involved electrons tunneling from the outermost STM tip atom to

the $O_2$ molecule under the tip, excitations induced by the tunneling current are confined to only one $O_2$ molecule (dimensions of ca. 1 Å). The spatial selectivity of tunneling induced dissociation of two adjacent $O_2$ molecules is shown in Fig. 4e-h. The tip was precisely positioned over the centre of the $O_2$ and the feedback loop used to maintain constant tunneling current was turned off. A voltage pulse (100 ms to 10 s) was then applied, and the current was monitored. Fig. 4f shows the current during a 0.3 V pulse with a sudden drop in current, highlighting the occurrence of the dissociation. A rescan of the same area in Fig. 4g shows the dissociated molecule with one oxygen atom on a face-centered cubic (fcc) site and the other on a hexagonal close-packed (hcp) site. The neighbouring molecule (5.54 Å away) was unaffected by the pulse. By positioning the tip over this molecule and applying a second pulse, dissociation was observed with the two oxygen atoms placed on hcp sites. The energy barrier for rupturing the O-O bond was calculated as 0.38 eV, which needed to be overcome with the energy transferred from one tunneling electron (0.4 V) or multiple tunneling electrons (two for 0.3 V, and three for 0.2 V). Such a vibration laddering climbing process is suitable for the mechanism of most inelastic tunneling dissociations.[41]

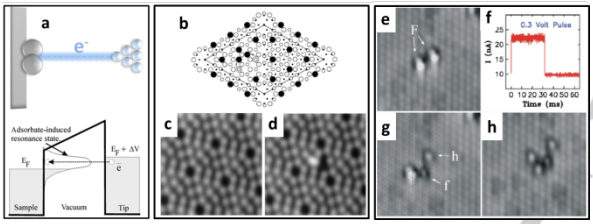


**Figure 4.** a) Schematic illustration of the inelastic electron tunneling dissociation process. Inelastic electrons are injected into the molecule through the adsorbate-induced resonance state. b-d) Displacement of Si adatoms on Si(111)-7×7 surface. STM images of the surface showing the site occupied by the two adatoms before (c) and after (d) transfer in the faulted half of the unit cell. Reproduced from Ref. [39] with the permissions of the American Physical Society. e-h) $O_2$ molecule dissociated on Pt(111) surface. e) STM image of two adjacent $O_2$ molecules adsorbed on fcc 3-fold hollow sites of Pt(111) at 50 K. f) Tunneling current *vs.* time during a 0.3 V pulse over the $O_2$ molecule on the right; sudden change at 30 ms is the moment of dissociation. g) STM image after dissociation showing one O atom on fcc site f, and the other on hcp site h. h) STM image taken after applying a second pulse over the remaining molecule, showing dissociation into two O atoms on hcp sites. Reproduced from Ref. [40] with the permissions of the American Physical Society.

In the case of $O_2$ on Ag(110), tunneling of electrons from the STM tip into the $O_2$ can be used to control the pathway of the dissociation, giving rise to two adsorbed O atoms separated along the [110] direction.[42] It was demonstrated that the molecule rotation occurred before the bond dissociation, therefore oxygen atoms were separated exclusively along the [110] direction, regardless of the alignment axis of the adsorbed $O_2$. In contrast, the ejection of electrons from the $O_2$ molecule produced adsorbed O atoms separated along the [001] direction. However, the dissociation of $O_2$ on Ag(100) surface took place at a high threshold bias voltage of +3.3 V, and the produced atom pairs showed a far range of motion by immediately pulling each other apart.[43]

Dissociation processes induced by inelastic electron tunneling are extremely popular among on-surface reactions; in light of this, atomic-scale knowledge of the dissociation of diatomic molecules is a prerequisite for understanding more complicated surface reactions. By tunneling electrons into a molecule at a specific position, the precise rupture of a bond can be attained, by eventually cleaving off unnecessary parts of a molecule, and generating active sites. The molecular fragments obtained may further be used as building blocks for new chemical species.

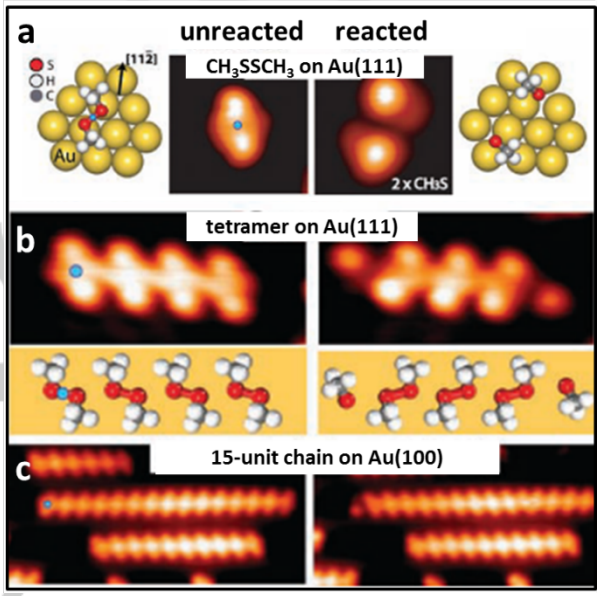


**Figure 5.** STM images and schematic models of $CH_3SSCH_3$ molecules before and after electron induced dissociation. a) Dissociation of $CH_3SSCH_3$ into two $CH_3S$ fragments by applying a pulse of 1.4 V. Chain reaction in b) $CH_3SSCH_3$ tetramer on Au(111) and c) 15-unit chain assemblies on Au(100) stimulated by a voltage pulse of 0.9 V on top of the terminal molecule (blue dot), leading to the synthesis of new $CH_3SSCH_3$ molecules of opposite conformation. Reproduced from Ref.[44b] with the permissions of The American Association for the Advancement of Science.

Several examples of selective bond breaking in polyatomic molecules *via* electrons tunneling have been discussed.[44] For example, Yates *et al.* investigated electron-induced reactions of linear dimethyldisulfide ($CH_3SSCH_3$) molecules bonded to Au(111) and Au(100) surfaces using STM at 5 K to inject electrons and image the reaction products.[44b] Single $CH_3SSCH_3$ molecules were adsorbed on Au surface in a *trans* conformation, i.e. with two methyl groups located at the two ends of the S-S bond adopting *trans* geometry. Fig. 5a shows that a single $CH_3SSCH_3$ molecule was dissociated into two equivalent $CH_3S$ fragments by firstly positioning the tip at the blue circle, and then by applying a voltage pulse (1.4 V) to inject tunneling electron into the S-S bond. In the self-assembled linear

structures, each molecule has the same orientation of the S-S bond and the same *trans* configuration of the two $CH_3$ groups.

The injection of tunneling electrons into the molecule at one end of the self-assembled chain led to a propagating chemical reaction along the molecular backbone. Interestingly, the newly obtained molecules had a mirror configuration compared with the original ones. Noteworthy, at a higher molecular coverage and at adsorption temperatures ranging between 70 K and 200 K, "linear" $CH_3SSCH_3$ chains up to five units in length were formed on the Au(111) surface.

A chain reaction could also be induced by applying electron pulses into $CH_3SSCH_3$ molecules self-assembled on Au surface. The chain reaction can be illustrated as a sequence of elementary steps ($CH_3S$ + $CH_3SSCH_3$ → $CH_3SSCH_3$ + $CH3_S$) and is being portrayed in Fig. 5b and 5c. This seminal work revealed that it is possible to synthesise desired products on surface *via* low-energy and stereospecific pathways. Ho and co-workers reported the multistep dehydrogenation of individual ethylene molecules adsorbed on Ni(110).[45] A voltage pulse between 1.1-1.5 V induced the dehydrogenation of ethylene first to acetylene and further to carbon atoms. Moreover, the electrons from STM tip could also be used to break a C-H bonds in a single acetylene molecule adsorbed on Cu(100),[46] or to dissociate individual pyridine and benzene molecules on Cu(100).[47]

One further challenge for tip-induced surface chemistry consists in breaking and forming chemical bond selectively in single complex organic molecule exhibiting a range of different functional groups. The bond energies of different covalent bonds in a single polyatomic molecule may be significantly different. In inelastic tunneling dissociation process, the probability of the electron energy transfer exponentially decreased with increasing bond energy.[48] The strong chemical bonds can be unaffected during the dissociation of the weak chemical bonds, which opens the way towards stepwise dissociation sequencing. For example, iodobenzene molecule exhibits three types of covalent bonds, i.e. C=C, C-H, and C-I, and their bond strength ratio in the gas phase was estimated as 3:2:1, respectively. [49] In case of iodobenzene adsorbed on Cu(111), the weakest C-I bond was firstly broken at a lower bias voltage of 1.5 V, and further dissociation of phenyl occurred as the bias voltage was raised above 3.1 V.

Ho *et al.* demonstrated that it is possible to stimulate a sequence of target- selective bond dissociation and formation steps in 1,4-bis(4'-(acetylthio)styryl)benzene (DSB-2S-2Ac) molecules adsorbed on a NiAl(110) surface at 12 K.[50] The four functional groups were dissociated one after the other by injection of electrons with different energies (by applying different bias voltages) at the precise locations (Fig. 6a). The threshold biases for removing acetyl groups and sulfur atoms were found to amount to 1.8 V and 2.4 V, respectively. These voltages were proved not being sufficient for breaking C-H and C-C bonds, thereby indicating the integrity of the aromatic back-bone of the molecule. The two sulfur functional groups produced by the selective dissociations of acetyl groups could be used as the reactive sites for further combination with Au adatoms. As monitored in Fig. 6b, the formation of Au-S bonds resulted in the conformational change of the aromatic backbone. The spatial map of the molecular resonance and the Au states in the DSB-2S-2Au complex (Fig. 6c) indicated that only one Au-S bond was covalent in nature and the orbital hybridization (coordination bond) between the other Au and S was localized.

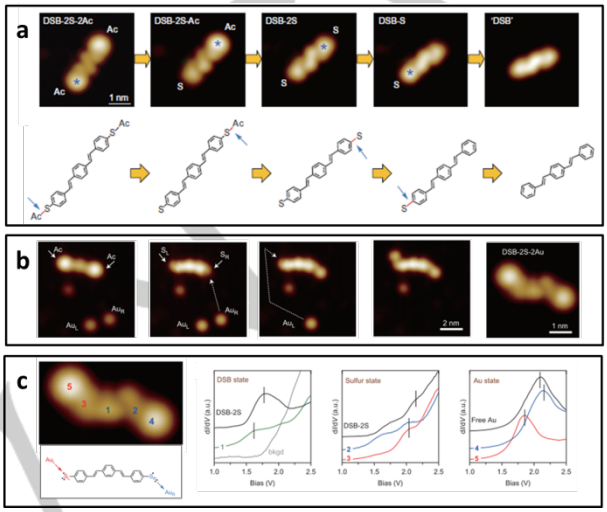


**Figure 6.** a) Stepwise dissociation sequence of the DSB-2S-2Ac molecule. b) Formation sequence of the DSB-2S-2Au complex. c) Spatially resolved spectroscopy of the DSB-2S-2Au complex. The dI/dV spectra taken at locations 1, 2, 3, 4 and 5 of the complex as indicated in the STM image show states of DSB, sulfur and Au. The spectra of DSB-2S and the isolated Au atoms before the association were shown for comparison. The energy state of middle part (1) was red shifted about 0.15 eV, which indicated the molecule connected with metal leads. The formation of strong DSB-2S-Au covalent bond was proved by the 0.25 eV red shift of $Au_L$ (5 marked in STM image) state and 0.1 eV red shift of $S_L$ (3 marked in STM image) state. The 50m eV slightly higher shift of $Au_R$ (4 marked in STM image) state caused by the weak coordination bond between $Au_R$ and $S_R$. Reproduced from Ref. [50] with the permissions of Springer Nature.

Intramolecular hydrogen atom transfer, also known as hydrogen tautomerization, is a key process occurring in photochromic and enzymatic reactions. By using STM, single molecule tautomerization induced by tunneling electron injection has been investigated, e.g. naphthalocyanine on a NaCl bilayer on Cu(111),[51] phthalocyanine[52] and porphyrin[53] on Ag(111). Moreover, the excitation mechanism of tip-induced tautomerization within a porphycene molecule was explored by Grill and co-workers.[54] On Cu(110),[54a] the porphycene molecule switched between two mirror-symmetric *cis* configurations in which two inner hydrogen atoms were transferred simultaneously. No *trans* configuration was observed during the experiment, suggesting that the *trans* tautomer was not sufficiently stable to be detected by STM. At a low experimental temperature of 5K, the appearance of porphycene molecules remained unchanged during scanning with low bias voltages, indicating that no tautomerization was induced thermally. However, the reversible *cis-to-cis*

tautomerization yield increased when raising the bias voltage above 200 mV. By measuring the tunneling current ($I$) dependence of the tautomerization rate ($R$) at various bias voltages, the $R$ was found to follow the power law of $R \propto I^n$, where $n$ was considered as the number of tunneling electrons needed for one molecule switching, thus enabling to identify the mechanism of such process as a vibrationally induced one. On Cu(111) the porphycene molecules adsorbed exclusively in its *trans* configuration with the two inner hydrogen atoms located on opposite pyrrole rings. [54b] At 5K, the unidirectional *trans-to-cis* and reversible *cis-to-cis* tautomerization were realized by applying a voltage pulse directly above molecule. A threshold voltage at ca. ±150 mV was required to trigger both processes, and identical behavior was exhibited for both bias polarities. Moreover, the unidirectional *trans-to-cis* process was also induced in a non-local fashion, and the conversion occurred on molecules located about 10 nm far from the tip manipulation position (electron injection point) by applying a voltage pulse of ±1.5 V. A hot carrier-mediated mechanism was proposed to explain this phenomenon, in which hot carriers (electrons or holes) generated from tip manipulation travelled along the surface to trigger the tautomerization remotely. Interestingly, the reversed *cis-to-trans* switching was never observed *via* tip excitation, but it took place when heating the surface up to 30 K. The *trans* tautomer was confirmed to be thermodynamically dominant on Cu(111), while the presence of *cis* tautomer was monitored on Cu(110). This indicative influence of the surface state provided a new approach to control the tautomerization behavior by modifying the local surroundings of a single molecule.[55] On Cu(110), a Cu adatom was precisely placed close proximity to a porphycene molecule ( 6 - 9 Å from the molecular center) *via* vertical manipulation, and the tautomerization rate of the molecule was adjusted effectively according to the location of adatom. Reversible tautomerization would be completely quenched, if one adatom was placed right next to the porphycene molecule (< 6 Å from the molecular center).

The Kondo effect arises from the coherent spin-flip scattering between the conduction electrons in a metal and the localized spins of magnetic impurities, resulting in a characteristic change in electrical resistivity at sufficiently low temperature. Owing to the high selectivity and atomic precision, STM manipulations provide a novel route to allow insight into the Kondo effect at the single molecule level. On-surface studies focus on the Kondo resonance state phenomenon *via* chemical control of magnetic molecules interacting with nonmagnetic surfaces. As representative molecular magnets, transition-metal containing metal phthalocyanine (MPc) molecules adsorption on 2D metallic surfaces have been extensively explored. The Kondo resonance was found to be tunable for FePc molecule on Au(111) by changing the molecular adsorption configurations, i.e. the on top and bridge configurations.[56] Different adsorption configurations influenced the symmetry of the ligand field through the local coordination to the substrate. According to the STS spectra recorded over the Fe atom, the calculated Kondo temperature was lower for on top configuration. Another example is represented by TBrPP-Co (TBrPP = 5,10,15,20-tetrakis(4- bromophenyl)porphyrin) on Cu(111), reported by Hla's group.[57] By applying 2.2 V voltage pulse, isolated TBrPP-Co molecule switched from "saddle" to "planar" adsorption conformation, reducing the distance between the central spin-active Co atom and the underlying Cu(111) substrate. STS spectra revealed that the switch of the molecular conformation enhanced spin-electron coupling, further increasing the associated Kondo temperature from 130K to 170K.

The Kondo effect exerted by an MPc molecule also depends on MPc's chemical composition. Zhao and co-workers reported that dehydrogenation process could turn on the Kondo effect of CoPc molecule on Au(111).[58] The initial CoPc molecule exhibited no Kondo effect, and removing eight hydrogen atoms with voltage pulses from a STM tip allowed the molecule to chemically bond to the Au substrate. The localized spin was recovered in this artificial structure. A clear Kondo resonance and a high Kondo temperature at 200 K were observed. The dehydrogenation threshold voltage applied was found in the range of 3.3 V to 3.5 V. In case of a FePc molecule adsorbed on Au(111), cutting away its eight outermost hydrogen atoms *via* applying -3.5 V voltage pulse turned off the Kondo effect.[59] The formation of the chemical bonds between the dehydrogenated CoPc molecule and Au atoms on surface increased the distance between $Fe^{2+}$ ion and Au atoms, weakening the Fe-Au coupling. Consequentially, the molecule changed from the Kondo state to the magnetic triplet state. Kim and co-workers demonstrated that the spin state of Co-porphyrin on Au(111) could be reversibly switched by binding and unbinding NO molecule.[60] The Kondo effect was switched off by the formation of coordination complex NO-Co-porphyrin, and could switch back on by unbinding of NO through local manipulation or thermal desorption (at 500K). DFT analysis explained the mechanism of this switching process, as the suppression of magnetic moment in NO-Co-porphyrin on Au surface. Similar experimental phenomena were investigated by Tsukuhara and co-workers.[61] CO and NO showed different impacts on the Kondo effects of FePc on Au(111). CO coordination caused the localized molecular spins disappear because of the change in the electron configuration by the CO-Fe bond formation. Meanwhile, NO coordination reduced Kondo resonance due to the reducing of the coupling of Fe and Au atoms.

Fu *et. al.* manipulated the Kondo resonance by placing individual MnPc molecule on silicon-supported Pd film.[62] The Kondo temperature was depended on the film thickness, and the lowest (23 K) and highest (419 K) Kondo temperature occurred at 15 and 17 monolayers, respectively. The oscillating Kondo temperatures were proved to be attributed to the formation of the thickness-dependent quantum-well states in the host Pb islands.

## 3. Molecular reactions: chemical bond formation

Chemical bond formation can be naively seen as the exact opposite to the bond dissociation. The simplest example of the STM induced chemical bond formation comprises the coordination between CO molecule and Fe atom accomplished *via* a vertical manipulation procedure, as reported by Lee and Ho.[63] Individual iron atoms were evaporated and frozen onto the Ag(110) surface at 13 K, and then CO molecules were transferred toward the Fe atoms by means of the STM tip, yielding the generation of Fe(CO) and $Fe(CO)_2$ complexes upon ramping the bias from -70 mV to -4 mV. The STM image in Fig. 7a suggests that in the reaction products CO ligands exhibit an inclined configuration in the Fe-Ag(110) system. This seminal work paved the way towards chemical bond formation *via* reactions induced with STM tip.

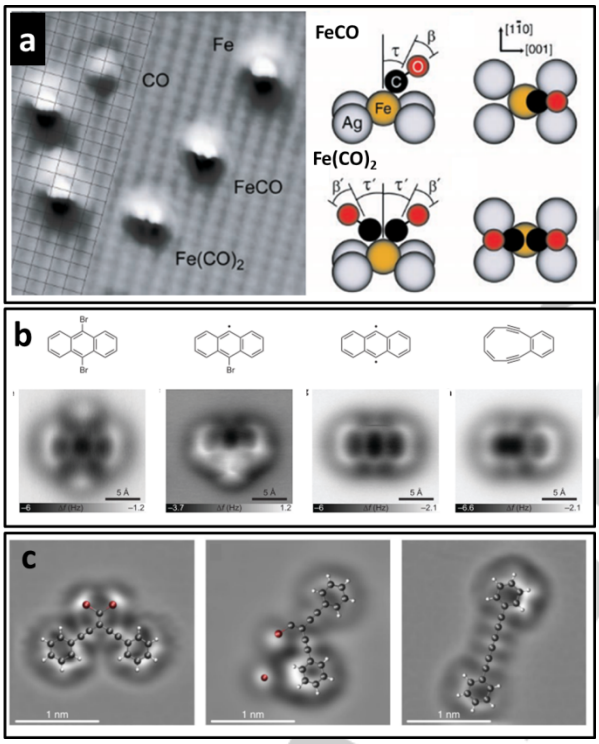


**Figure 7.** a) Atomically resolved STM image containing Fe, CO, FeCO and $Fe(CO)_2$. A grid was drawn through the Ag(110) surface atoms to guide the determination of the adsorption sites. The models of side view and top view of Fe(CO) and $Fe(CO)_2$ shown the CO to be tilted by angle $\tau$ and bent by angle $\beta$. Reproduced from Ref. [63] with the permissions of The American Association for the Advancement of Science. b) Structures and nc-AFM images of the starting molecule and the reaction products formed by tip-induced debromination and subsequent retro-Bergman cyclization. Reproduced from Ref. [67] with the permissions of Springer Nature. c) Corresponding Laplace-filtered AFM images with structural ball-and-stick models of 1,1-dibromo alkene, intermediate radical and triyne molecules. Grey, red and white balls represent C, Br and H, respectively. Reproduced from Ref. [69] with the permissions of Springer Nature.

The groups of Hecht and Grill reported the lateral manipulation of porphyrin molecules on Au(111).[64] Different molecular appearances in the STM imaging were observed by comparing porphyrins bonded by a coordination bond with single gold adatoms underneath the molecular monolayer with unbonded ones. Such tuning of the single molecules electronics has been ascribed to an electrostatic shift of adsorbate-induced electronic state. Repp and co-workers brought one gold adatom into close contact with one pentacene molecule *via* tip manipulation.[65] New metal atom-molecule bond were formed by resonant inelastic electron tunneling through the lowest unoccupied orbital of pentacene, and imaged by STM as changes in bond hybridization.

Intramolecular reaction induced by inelastic tunneling electrons was first reported by Kim and co-workers.[66] 1,3-butadiene molecule was synthesized on a Pd(110) surface *via* the dissociation of C–H bonds of *trans*-2-butene molecule. The threshold voltage for this reaction was estimated as 365 mV, and could coincide well with the vibrational excitation of the C-H stretching mode. Another example is the reversible Bergman cyclization reported by Gross and co-workers.[67] Towards this end, 9,10-dibromoanthracene (DBA) molecules were deposited on a Cu(111) surface partially covered by two monolayers of NaCl. The two C-Br bonds of DBA were cleaved by applying two voltage pulse (3.3 V) to obtain the diradical. Subsequently, another voltage pulse of 1.7 V was applied above this diradical, yielding a new molecule consisting of fused six- and ten-membered rings, and it was ascribed to the formation of diyne by hemolytic cleavage of the C–C bond shared by two fused benzene rings.

The ultrathin NaCl film employed as substrate facilitated the stabilization of diradical and diyne, yet reversibility between these two forms was observed. The atomically resolved non-contact atomic force microscopy (nc-AFM) images displayed in Fig. 7b offer a genuine evidence of the products in each manipulation step.

Recently, Peña and collaborators explored a route towards formation of cyclic acenes by STM/AFM tip manipulations.[68] The tetraepoxycyclacenes with 8 and 10 units were synthesized and subsequently deposited onto Cu(111) surface. The on-surface deoxygenation step of tetraepoxycyclacenes and formation of corresponding cyclacenes was accomplished *via* either scanning the tip on the top of the molecular island at large bias (2.5-3.4 V) or by applying single voltage pulses above one molecule, which changed the shape and symmetry of the molecular cavity. The nc-AFM images enabled to picture the two main products: 'D'-shaped with two neighbouring epoxy groups being deoxygenated, and 'oval'-shaped with two opposite epoxy groups deoxygenated. Noteworthy, the deoxygenation process altered the hybridization state of the two carbon atoms of the corresponding epoxy group from $sp^3$ to $sp^2$, generating curved aromatic molecules.

Moreover, the mechanisms of Fritsch-Buttenberg-Wiechell rearrangement were demonstrated by Gross and co-workers.[69] Different voltage pulses were applied to cleave the two C-Br bonds of dibromoalkene one by one. These two debromination were carried out by applying voltage pulses of 2.5 V and 2.8 V,

respectively. Such dehalogenation triggered the rearrangement of the molecular backbone into linear polyynes. The geometry of reactants, intermediates and final products were monitored by nc-AFM, as portrayed in Fig. 7c. In case of Cu surface, this reaction resulted in the formation of carbine radicals, which were found to immediately bond to the underlying Cu atom and blocked the rearrangement process. Unfortunately, the observations on bilayer NaCl on Cu(111) surface failed to detect a long-lived carbene intermediate. The structural insight into the unexpected bromo-vinyl radical intermediates revealed that the C=C˙-Br unit was nonlinear. This successful control of skeletal rearrangements by atom manipulation could open new pathways for the synthesis of carbon-rich materials.

On-surface chemical bond formation between two molecular fragments involves more complex mechanisms. The two molecular fragments have to be in close enough to physically overlap the electronic wave functions of the reactive groups, which must align properly to form a bond between them. In some cases, such groups first get bonded to the metal substrate after dissociation from a parent molecule. For example, in phenyls produced by deiodination of $C_6H_5I$, the free C bonded to flat Cu surface with a tilted angle of 45°,[70] which has been proved as one intermediate state during tip-induced Ullmann reaction. Ullmann reaction has gathered much attention because of its efficiency for linking aromatic units through C-C covalent bonds. In his seminal work, Hla *et al.* demonstrated the on-surface Ullmann reaction by multistep STM manipulation [71] (Fig. 8a). In a low-temperature set-up (4 K), the STM tip first injected a 1.5 eV tunneling electron into each iodobenzene molecule. This operation induced C-I bonds cleavage yielding free phenyl radicals. While in solutions these are extremely reactive species, on a conducting surface they get stabilized by the combination of π-π interaction with the underlying substrate and σ-interaction with the Cu atoms at the lower part of the Cu(111) step edges. Subsequently, the two phenyl radicals were slided and brought into close proximity (in head to head fashion). Upon applying a positive voltage pulse of 0.5 V, covalent coupling between these two phenyl radicals was prompted yielding to biphenyl.

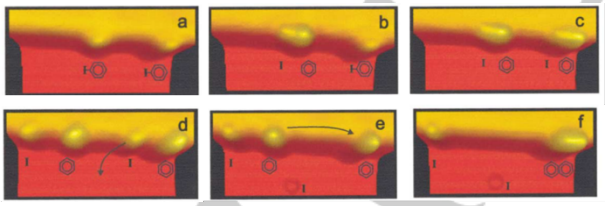


**Figure 8.** STM images (70×30 Å²) showing the initial steps of the tip-induced Ullmann synthesis. a) Two iodobenzene molecules were adsorbed at a Cu(111) step edge. b,c) Electron-induced selective dissociation of iodine from both molecules. d) Removal of the iodine atom to a terrace site by lateral manipulation. e) Bringing together two phenyls by lateral manipulation. f) Electron-induced chemical association of the phenyl couple to biphenyl. Reproduced from Ref. [71] with the permissions of American Physical Society.

Recently, Rosei *et al.* synthesized organometallic oligomers *via* the tip-induced C-H activation of tetrathienoanthracene (TTA) molecules on Cu(111).[72] After applying voltage pulses (above 3 V), the molecules organized into a more densely packed arrangement compared to the spontaneously self-assembled structure. Based on the average contour length of 1.43 ± 0.06 nm between the centers of mass of two neighbouring molecules, the products were identified as organometallics *via* the formation of C-Cu-C bond. This reaction process was found being substrate dependent, as demonstrated by the absence of oligomerization when Au or highly oriented pyrolytic graphite (HOPG) was employed as surface. Compared with the similar oligomers obtained *via* thermo-induced on-surface Ullmann reaction,[73] this method allows the precise spatial control, and at the same time, can eliminate the formation of by-products.

By tailoring the precursor structures, Ullmann reaction can also be controlled with atomic precision. Grill, Hecht and co-workers generated tetraphenylporphyrin(TPP) dimers, 1D chains and 2D networks on Au(111) by adjusting the number and position of Br substitutions exposed on a TPP core.[74] Moreover, by taking advantage of the energy barrier difference between C-Br and C-I bonds, highly regulated covalent networks were obtained followed a hierarchical reaction route (Fig. 9a-c).[75] The precursor *trans*-$Br_2I_2$TPP, equipped with two bromine and two iodine substituents at orthogonal terminal sites, were first coupled into linear structure by cleaving I atoms at 393 K, and subsequent formation of the 2D network by combining the linear chains at 523 K *via* C-Br bonds activation. Noteworthy, such step-wise approach compared with one-step growth procedure resulted in a decreased number of defects within the obtained 2D networks. Such hierarchical approach was more effective, because of the presence of active sites equally spaced along the pre-synthesized TPP polymer chain. Once the first inter-chain C-C bond was formed, the neighbouring active sites could be automatically arranged for the next C-C bond formation.

Graphene nanoribbons (GNR) synthesis *via bottom-up* approach has attracted recently considerable attention in the community as it can be exploited for controlling the width and edge structures at atomic precision as a route to open a bad gap in graphene.[76] In this on-surface synthesis process, Ullmann coupling acts as an important step allowing formation of the embryonic form of the targeted GNR.[77] In 2010, the groups of Fasel and Müllen first built a prototypical armchair GNR with width of 7 carbon atoms (7-AGNR) on Au(111).[78] As displayed in Fig. 9d-f, the 7-AGNR was formed from 10,10'-dibromo-9,9'-bianthryl (DBBA) monomers *via* two-step reactions: Ullmann coupling and subsequent cyclodehydrogenation. In the first step, Ullmann-type oligomerization between DBBA monomers took place to generate linear polyethylene chains at 473 K; second step, consisted in an increase of the surface temperature up to 673 K to trigger intramolecular cycledehydrogenations, resulting in the planar GNR structure *via* C-C coupling. Based on this two-step reaction, various precursors were designed to synthesize AGNRs with fine-tuned width. Metallic 5-AGNR (3p+2 type, here p=1) was synthesized by both Liljeroth's[79] and Chi's[80] groups *from* different precursors, and semiconducting 6-AGNR (3p type, here p=2) and 13-AGNR (3p+1 type, here p=4) were obtained by Sambi's[81] and Crommie's[82] groups, respectively. The

theoretical studies indicated that the band gap of 3p type and 3p+1 type GNRs was closely related to the nanoribbon width.[83] 13-AGNR showed a smaller band gap than 7-AGNR in the STS spectrum,[82] suggesting that increasing the width of the nanoribbon could result in more similar electrical properties to 2D graphene. Noteworthy, nanostructures with *zig-zag* edges are expected to exhibit spin polarized electronic edge states. However, the formation of GNR with *zig-zag* edges is almost impossible in solution-mediated reactions due to their relatively unstable nature. Remarkably, under the UHV conditions, Fasel's group reported the first synthesis of full *zig-zag*-edged GNR (ZGNR) using U-shipped monomers.[84] Because of the strong chemical reactivity at the nanoribbon edges, this 6-ZGNR was found to be strongly bounded to underlying Au(111) surface, which limits its application at ambient conditions. The edge passivation approaches could be provided to reduce the chemical reactivity, at the same time, to preserve the electronic properties of the pristine GRNs. Some hybrid-edge structures have been obtained with properly designed precursors, such as chevron-types,[85] chiral-types,[86] and acene-types.[87] Recently, new type *zig-zag* edge-extended GNRs with a width of 9 up to 11 carbon atoms was derived from *zig-zag* edge-encased poly(para-2,9-dibenzo[bc,kl]coronenylene) polymer chains, exhibiting a high radio of *zig-zag* (67%) *vs*. armchair (25%) edge segments.[88] Furthermore, the addition of heteroatom dopants into GNR represents another efficient approach to modulate GNR's band structure and electronic properties. In particular, N-substituted precursors were first introduced to synthesize N-doped GNRs.[89] The further combination of N-substituted precursors with pristine hydrocarbon precursors resulted in partially doped GNR heterostructures, which performed similar behaviour as traditional *p-n* junctions. Hitherto, a series heteroatom doped GNRs have been fabricated *via bottom-up* synthesis: e.g. B-doped AGNR[90], S-doped chevron-type GNR[91], and OBO-doped chiral GNR[92]. Remarkably, Ma *et al.* demonstrated the fabrication of heterostructures in 7-AGNR by 'direct writing' with STM tip.[93] The intra-ribbon heterostructures consisted the intermediate segment that had only one side of the polyanthrylene converted to the 7-AGNR structure while the other side remains in the polymeric structure. By applying a pulse of -2.0V for 30 ms, one unit cell of an intermediate segment could be converted to GNR. Through this procedure, multiple GNR/intermediate heterostructures at selected molecular sites could be fabricated. The intermediate segment embedded in one GNR performed like a quantum dot confined in a double-barrier structure.

While all examples presented so far refer to experiments carried out in UHV and at low temperature (i.e. a few Kelvin), manipulation of molecular arrays can be explored at room temperature at the interface between a solid substrate and a supernatant solution. The spontaneous self-assembly of functionalized molecules can result in high-ordered and large-area nanostructured surfaces. Starting with such pre-assembled structures, polymers with multiple units can be generated through tip-induced bond formation. A beautiful example was reported by Okawa and Aono by using the STM tip to write directly on a HOPG surface 1D polydiacetylene nanowire.[94] An artificial defect was first created on tightly-packed 10,12-nonacosadiynoic acid (NCDA) monolayer by applying a positive voltage pulse of +5 V. Subsequently, the tip was scanned from top to bottom of the image with applying a negative bias of -4 V. The central diacetylene units of NCDA underwent polymerization through a chain reaction mechanism initiated by the formation of a diradical. One polydiacetylene nanowire was formed between the initial position of the tip and the artificial defect, generating a bright line in the STM image (Fig. 10a). Noteworthy, the authors demonstrated a 1 nm spatial precision in initiating and terminating the linear propagation at any chosen point.

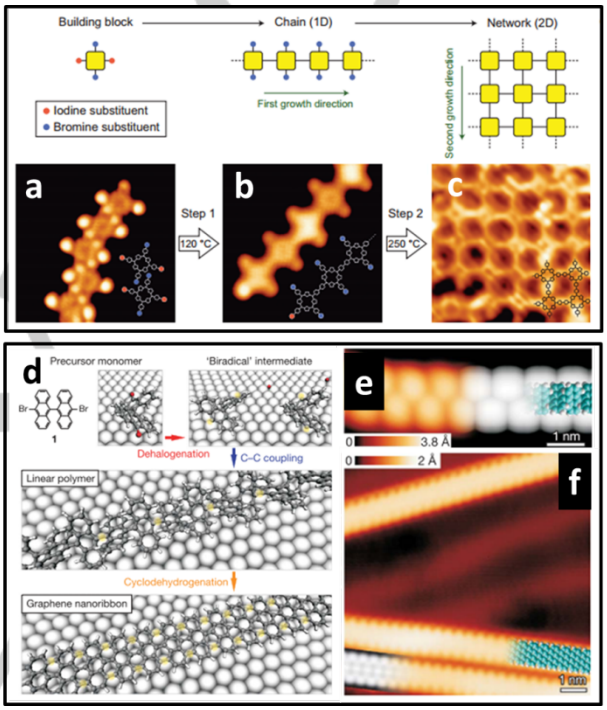


**Figure 9.** a-c) Hierarchical growth following sequential thermal activation, and schematic illustration of this two-step Ullmann reaction. STM images of (a) *trans*-$Br_2I_2$TPP molecules deposited on Au(111) at 80 K, (b) debromination at 393 K. (c) deiodination at 523K. Reproduced from Ref. [75] with the permissions of Springer Nature. d-f) *Bottom-up* fabrication of atomically precise GNRs on Au(111). (d) Schematic illustration of the synthesis strategy. High-resolution STM image of (e) a polyanthrylene chain after dehalogenation at 473 K, and (f) STM image of the 7-AGNRs after cyclodehydrogenation at 673 K. DFT simulations of the STM images shown in the right side. Reproduced from Ref. [78] with the permissions of Springer Nature.

Polymerization of self-assembled diacetylene monomers on surfaces and interfaces has been studied in details over the past years.[95] Activation approaches involving UV light irradiation or tip-induced polymerization have been employed to create conjugated polydiacetylene molecules.[96] Nevertheless, despite a high spatial selectivity over polymer initiation, the polymerization termination step is still poorly controlled, and thus the resulting length of the polydiacetylene polymers is often random. Noteworthy, it has been demonstrated recently, that the

conjugated polydiacetylene polymers with well-defined lengths can be fabricated by confining the liquid–solid molecular self-assembly of 10,12-pentacosadiynoic acid (PCDA) within nano-corrals created in chemically modified HOPG (CM-HOPG). To this end, De Feyter and co-workers covalently modified the HOPG surface using an electrochemical grafting procedure with an aqueous solution containing *in situ* generated 3,5-bis-*tert*-butylbenzenediazonium cations.[97]

Subsequently, nanocorrals were created within the dense monolayer of covalently attached aryls by raster scanning the desired area with the STM tip at high current ($I_t$ = 200 pA) and low sample bias ($V_s$ = -1mV). In the next step, a droplet of PCDA in 1-phenyloctane was drop-casted on top of CM-HOPG surface and topochemical polymerization reaction was initiated with a local electrical pulse from the STM tip (-3.8 V for 100 µs), allowing the formation of arrays composed of polymerized species with desired dimensions.

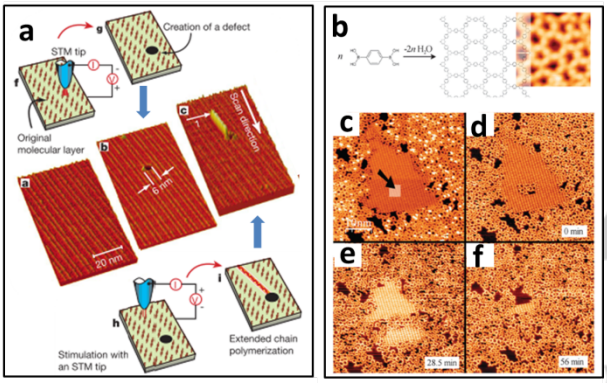


**Figure 10.** a) STM images and diagrams showing the process of controlling the initiation and termination of linear chain polymerization with an STM tip. Reproduced from Ref. [94] with the permissions of Springer Nature. b) Tip-induced polymerization of BDBA. c) The STM tip was brought very close to the H-bonded layer and scanned over a small area at the position indicated by the arrow. (d) The polymerization reaction was immediately initiated. (e&f) and slowly propagated until complete disappearance of the H-bonded phase. Reproduced from Ref. [98] with the permissions of The Royal Society of Chemistry.

As polymeric diacetylenes are being predominantly used as conductive materials, such precise control over nanoscale fabrication could advance the fabrication of novel molecular nanoelectronic devices, with geometries at will.

2D covalent framework fabricated *via* atom manipulation was reported by Porte and co-workers.[98] The 1,4-benzenediboronic acid (BDBA) spontaneously self-assembled on Ag(100) assisted by hydrogen bonding. By positioning the STM tip very close to the self-assembled monolayer (-0.5 V, 10 nA) and scanning over a small area (25 $nm^2$), the self-assembled structure was disturbed, and dehydration condensation was initiated locally, as shown in Fig. 10b-f. Upon decreasing the tunneling resistance the mechanical interaction between tip and monolayer was enhanced, thereby triggering the generation of a polymerization nucleus. About 20% of the molecules desorbed from the surface during the dehydration, which conveyed necessary free room for the rearrangement of the remaining molecules (radicals). From the dense H-bonded pattern to the loose polymer phase, the reaction kinetics was affected by tip manipulation *via* steric effects. Strong electron irradiation with 15 eV E-beam was used to greatly accelerate the reaction kinetics in the polymerization of diboronic molecules.

## 4. Tip-induced vertical reactions

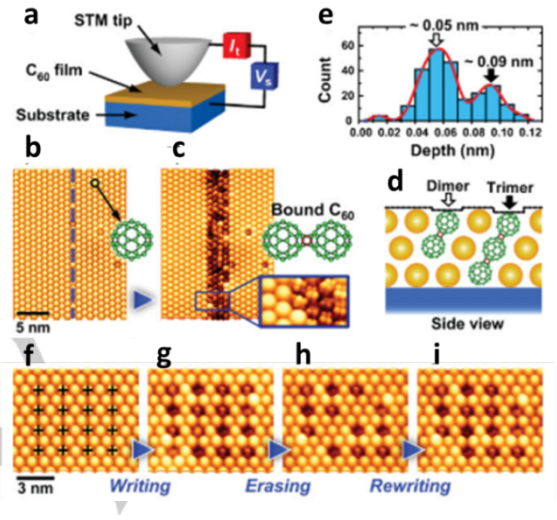


**Figure 11.** Control of unbound and bound states of $C_{60}$ molecules by an STM tip. a) Experimental setup. b) STM images of a three-layer-thick $C_{60}$ film. c) STM image after manipulation. The tip was scanned along the dotted line in (b) at a speed of 60 nm $s^{-1}$ with applying a sample bias of -3.5 V. Two $C_{60}$ molecules bound via the [2+2] cycloadditive four-membered ring was schematically shown. d) Histogram of depth of bound $C_{60}$ molecules relative to surrounding pristine $C_{60}$ molecules. e) Schematic side view of $C_{60}$ dimer and trimer. f–i) STM images of a $C_{60}$ film showing that single-molecule-level writing (f to g), erasing (g to h), and rewriting (h to i) of binary data. Reproduced from Ref. [102] with the permissions of WILEY-VCH Verlag GmbH & Co. KGaA, Weinheim.

As introduced in Section 3, the catalytic effect of the metallic substrates is essential towards high efficiency in diverse on-surface reactions. However, some reactions require to be stimulated by applying suitable bias voltage, i.e. the underlying metallic substrate operates as a chemically inert support. In this case, the tip-induced reactions can occur in the direction perpendicular to the surface. One typical example is the [2+2] cycloaddition of $C_{60}$ molecules, which has been first observed by Zhao *et al.*[99]. The tunneling of electrons (3 eV) from tip to neat $C_{60}$ films induced the cycloaddition reaction on GaAs(110) surface. More recently, Nakamura's group found that both polymerization and depolymerization of fullerenes could be achieved by injecting either holes or electrons into $C_{60}$ molecules.[100] Additionally, they compared $C_{60}$ behaviour on HOPG and Si(111) surfaces,[101] and found that the reaction spread was generally smaller in $C_{60}$ films grown on HOPG substrates. In $C_{60}$/HOPG films, the crystals had a larger

intermolecular separation and hence the smaller transfer matrix for electron transport than in $C_{60}$/Si(111) films, which could further support the band propagation hypothesis[100]. With direct observation on individual molecular reactions by STM, the polymerization and decomposition rates were found being proportional to the tunneling current, implying that each reaction was triggered by a single electron. One theoretical model was proposed suggesting that one tunneling electron injected into $C_{60}$ film could propagate in the electronic band of $C_{60}$ crystal, until it reached a specific site to cause the ionically enhanced cycloaddition reaction. Since the bound and unbound state of $C_{60}$ molecules could be controlled reversibly at the single-molecule level, topochemical data storage with this tip-induced reaction method may be explored to form a bit size of 1 nm (a single $C_{60}$ molecule).[102] As displayed in Fig. 11, $C_{60}$ film with a thickness of three molecular layers was prepared on a Si(111)-Ag substrate. The STM tip was then scanned along the dotted line (Fig. 11b) with a large negative bias voltage of -3.5 V.

As a result, tip-induced vertical oligomerization of $C_{60}$ molecules occurred near the scan line (Fig. 11c), and the dark $C_{60}$ molecules indicated their thermal rotation was suppressed due to chemical bonding with neighbouring molecules. As the STM image contract of the molecule could be altered by its vertical displacement, two shades related to pristine $C_{60}$ molecules might indicate different products. In Fig. 11e, two peaks at 0.05 nm and 0.09 nm were present in the histogram of the depth of dark $C_{60}$ molecules, in agreement with the vertical depressions for dimer and trimer, respectively. The single-molecule level topochemical data storage was performed as in Fig. 11f-i. The data writing (Fig. 11i-g) process realized by applying a negative bias (-2.0 V) above the cross-marked $C_{60}$ molecules one after another. The topochemical stored data were recorded by the displaced downward of $C_{60}$ due to dimerization or trimerization, which could be read-out by scanning with a fixed height to monitor the variation of current. Further, the dimerization/trimerization was found to dominantly take place with a smaller/larger electric field induced by the tip, which could offer an opportunity to increase the data density by a multistate bit operation. It was demonstrated that each bit could be a three-state memory bit by controlling the formation of the dimer and trimer. To erase the data (Fig. 11g-h), the STM tip was placed above the four dark $C_{60}$ molecules on a diagonal, and then a positive bias of +3.5 V. The bounded $C_{60}$ oligomers were dissolved into individual molecules, which recovered the same image contrast as the unreacted molecules around. Furthermore, the same position could be rewritten by applying a negative bias of -2.0 V again (Fig. 11h-j). This writing-erasing-rewriting cycle showed excellent reproducibility of this topochemical data storage method.

Diels–Alder (D-A) reaction between a conjugated diene and a substituted alkene (dienophile), is a prototypical electrocyclic reaction that can result in a formation of a six-number ring. Theoretical studies by Shaik's group predicted that the reaction barrier height could be reduced by applying an external electric field.[103] This theory was experimentally proven by Coote and co-workers *via* a tip-induced electrostatic catalysis of an on-surface D-A reaction.[104] As shown in Fig. 12a, the diene (surface tethered furan derivative) molecule were grafted to the STM gold tip through Au-S bond formation, while the non-polar dienophile (norbornylogous bridge with a terminal double bond) molecule packed edge-on on a flat Au surface *via* two parallel $CH_2S$-Au bonds. The D-A reaction between diene and dienophile was revealed by monitoring the tunneling current (Fig. 12b). In Fig. 12c, the frequency of current jumps remained constants over a wide range of positive bias voltages. On the contrary, at negative bias voltages this frequency increased from 5 $h^{-1}$ (-0.05 V) to 25 $h^{-1}$ (-0.75 V). By applying negative bias an external electric field oriented from STM tip to surface ($E_{surface}$< 0) was generated, yielding an acceleration of the D-A reaction rate by a maximal fivefold increase. The ability to control reaction kinetics and thermodynamics by the tip-induced electric field offers a new pathway towards heterogeneous catalysis, and can be employed to catalyse the non-redox chemical reactions.

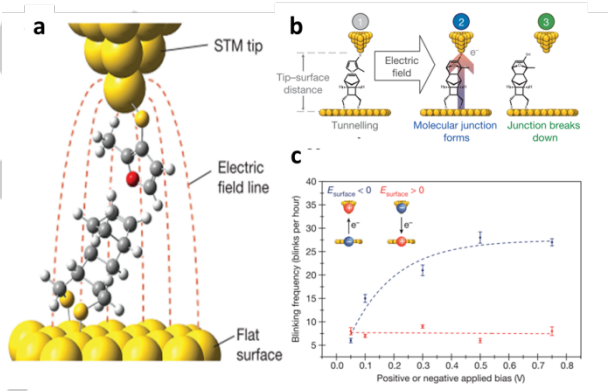


**Figure 12.** a) Reactants chemisorbed mode showing the norbornylogous bridge orientation with respect to the surface and to the electric field lines. b) The stages encountered during electrostatic catalysis of a Diels–Alder reaction. A negative electric field was applied to improve the reaction rate. c) Frequency of current jumps as a function of applied bias. Positive and negative biases were plotted in red and blue, respectively. Reproduced from Ref. [104] with the permissions of Springer Nature.

Device-oriented molecular manipulation using the STM tip and formation of nanoscale electronic circuits have been major subjects in Aono's group.[105] The nanoscale precise electrical wiring for molecular electronics was realized by tip-induced polymerization of aligned diacetylene molecules, yielding in conductive polyacetylene (PDA) wires in a defined direction. As connecting functional molecules with conductive nanowires is key to single-molecule electronics, the second step of this STM electrical wiring process should involve "chemical reshuffling" at the molecular level. Towards this end, a few phthalocyanine ($H_2Pc$) molecules were deposited on the self-assembled monolayer of diacetylene derivatives.[105a] in a polymer growth triggered by the STM tip (-3.8 V for 5 μs), one PDA nanowire was fabricated whose length extended until it reached a $H_2Pc$ molecule. Since the front edge of PDA polymerization had a

reactive carbene species, the PDA wire reacted with the encountered $H_2Pc$ to form C-C covalent bond *via* insertion reaction to the C-H bond on phenyl. Subsequently, the covalent connection of a single $H_2Pc$ molecule onto PDA conductive wire was realized. Moreover, a molecular-resonant-tunneling diode (RTD) was created by two PDA wires connecting to a single phthalocyanine molecule. In RTD, electron can directly tunnel through the phthalocyanine molecule only if the applied bias voltage matches the energy level of the molecule. It is noteworthy that the energy levels of phthalocyanine could be adjusted by selecting central metal atoms or substituents,[106] further affecting the switching properties of such molecular RTD device. By exploiting a similar approach, the same research group further fabricated a nanojunction between $C_{60}$ molecule and PDA conductive wire.[105b] This molecular soldering process was achieved *via* cycloaddition reaction between the propagating forefront part of the π-conjugated PDA backbone and a single $C_{60}$ molecule adsorbed on the surface. The covalent interaction in the $C_{60}$-PDA nanojunction was considered to reduce the energy gap of $C_{60}$ molecule. Based on these two examples, artificial fabrication of nanoscale electronic circuitry with required functional molecules at desired place could be successfully realized.

## 5. Conclusion and perspective

The tremendous pace in the improvement of scanning probe microscopies capabilities enabling the accurate control over the tip-sample junction made it possible to achieve atomically precise manipulation of matter. Nowadays, single atom/molecule manipulation *via* STM tip enables the formation of complex patterns and most importantly to explore new fundamental physics and chemistry at the atomic scale. Construction of atomic scale structures, such as quantum corrals and electron resonators, allowed *in situ* studies of quantum phenomena. However, the underlying of physical and chemical properties behind single atom and molecule are far from being fully unravelled. For example, the critical size of quantum phenomena and the formation of Kondo effect are still insufficiently explored.

STM manipulation technique extends the applications of scanning probe microscope and has become a powerful analytical approach in nanoscience. Stimulating chemical reaction at atom level provides distinctive insight into the reaction mechanism, which could give us unprecedented understandings of chemistry. As the STM image solely provides a map of the local density of electronic states, it does not offer a compositionally resolved picture of a molecular structure. More advanced techniques such as nc-AFM emerged more recently as powerful tools for the direct visualization of the chemical structures, especially when exploring intramolecular reactions.[107] Small changes of molecular structures during reaction processes, which can hardly be distinguished by STM imaging, can easily be captured *via* nc-AFM. The bond making and bond breaking processes can be monitored by the 'wire-frame' chemical structures of the intermediates.

Nowadays, a very limited number of the large arsenal of solution phase reactions have been realized on surfaces, and among them only a few could be induced by the STM tip. The tip-induced on surface reactions: Ullman coupling, Bergman cyclization, [2+2] cycloaddition, Fritsch-Buttenberg-Wiechell rearrangement, boronic acid condensation, Diels–Alder reaction and diacetylene polymerization, have been highlighted in this review. These pioneering works indicate that the advances in this tip-induced processes make it possible to *see* the structure and dynamics of single reactant, thus providing a new approach to study chemical reactions at the spatial limit. As many reaction mechanisms are still somehow speculative, it is highly expected that this new approach could provide supports to overcome these challenges. In particular, the introduction of multi-molecular reactions and more complex ensemble effects should be demonstrated.

Under the influence of STM tip, new chemical reaction pathways could be discovered on catalytic metal surfaces. The additional electric field as well as the electron injection may cause reactions that otherwise can't spontaneously occur in nature by tilting reactivity landscapes to favour one product over the other. In the STM manipulation process, STM tip is used as an engineering tool to trigger basic reaction building blocks, to bring them together in an assembled manner, and to connect them yielding new molecules. With selective bond breaking, the building blocks for synthesis of new molecules can be designed. The unnecessary part of the reactant can be cleaved to create active sites, and individual molecules may also be constructed for the assembly of larger molecule. On the longer term, the synthesis of individual human-made molecules, never seen in nature or realized *via* wet chemistry,[108] could be developed with tip-induced process.

It is certain that the STM manipulation will greatly contribute to nanoscience and nanotech industry, with an impact similar to that of STM imaging and spectroscopy during the last three decades. Molecules with specific functions can be constructed for the emergence of a new generation of nanoelectronic devices exhibiting complex functions, and further their physical and chemical properties can be studied in situ with spectroscopy techniques. With the realization of room temperature manipulation (in case of large molecules) and automated-tip-induced process (substantially increased the atomistic construction speed), the direct industrial application of the single-molecule construction could be possible in the foreseeable future. Additionally, tip-induced molecular assembly and reaction in a desired pattern has been performed as the smallest scale of nanoarchitectonics, which is introduced as a rising tide within current nanomaterial science. Indeed, manipulation of single molecule is an advanced research subject at the forefront of this research field.

By learning and capitalizing on the previous works, new avenues for future research in STM manipulation can emerge. One direction is to explore the basic laws of physics and chemistry in nature at the atomic level. Another direction is the synthesis nano-materials with properties for further applications in nano-electronics, such as novel functional molecules, conductive 1D, 2D and 3D polymers, and vertical artificial

structures. Finally, it should be noted that the rapid improvement of experimental technology might open an entirely new dimension for the atom manipulation technique, towards harnessing of structural and functional complexity in molecules-based materials.

## Acknowledgements

We acknowledge funding from the Agence Nationale de la Recherche through the Labex projects CSC (ANR-10-LABX-0026 CSC) and NIE (ANR-11-LABX-0058 NIE) within the Investissement d'Avenir program (ANR-10-120 IDEX-0002-02), and the International Center for Frontier Research in Chemistry (icFRC).

**Keywords:** STM • tip-induced • atom manipulation • chemical reaction • nanoscience

[1] P. S. Cohen, S. M. Cohen, *J. Chem. Educ.* **1996**, *73*, 883-886.
[2] R. B. Woodward, *Pure Appl. Chem., 33*, **1973**, 145-178.
[3] J.-M. Lehn, *Chem. Soc. Rev.* **2007**, *36*, 151-160.
[4] K. Ariga, J. Li, J. Fei, Q. Ji, J. P. Hill, *Adv. Mater.* **2016**, *28*, 1251-1286.
[5] G. Binnig, H. Rohrer, C. Gerber, E. Weibel, *Phys. Rev. Lett.* **1982**, *49*, 57-61.
[6] P. Avouris, *Acc. Chem. Res.* **1995**, *28*, 95-102.
[7] O. Marti, G. Binnig, H. Rohrer, H. Salemink, *Surf. Sci.* **1987**, *181*, 230-234.
[8] D. M. Eigler, E. K. Schweizer, *Nature* **1990**, *344*, 524-526.
[9] J. A. Stroscio, D. M. Eigler, *Science* **1991**, *254*, 1319-1326.
[10] a) P. Zeppenfeld, C. P. Lutz, D. M. Eigler, *Ultramicroscopy* **1992**, *42-44*, 128-133. b) K. F. Braun, K. H. Rieder, *Phys. Rev. Lett.* **2002**, *88*, 096801
[11] M. F. Crommie, C. P. Lutz, D. M. Eigler, *Science* **1993**, *262*, 218-220.
[12] M. T. Cuberes, R. R. Schlittler, J. K. Gimzewski, *Appl. Phys. Lett.* **1996**, *69*, 3016-3018.
[13] T. A. Jung, R. R. Schlittler, J. K. Gimzewski, H. Tang, C. Joachim, *Science* **1996**, *271*, 181-184.
[14] L. Bartels, G. Meyer, K. H. Rieder, *Phys. Rev. Lett.* **1997**, *79*, 697-700.
[15] D. M. Eigler, C. P. Lutz, W. E. Rudge, *Nature* **1991**, *352*, 600-603.
[16] T. C. Shen, C. Wang, G. C. Abeln, J. R. Tucker, J. W. Lyding, P. Avouris, R. E. Walkup, *Science* **1995**, *268*, 1590-1592.
[17] P. Avouris, R. E. Walkup, A. R. Rossi, T. C. Shen, G. C. Abeln, J. R. Tucker, J. W. Lyding, *Chem. Phys. Lett.* **1996**, *257*, 148-154.
[18] L. Bartels, G. Meyer, K. H. Rieder, *Appl. Phys. Lett.* **1997**, *71*, 213-215.
[19] L. Bartels, G. Meyer, K. H. Rieder, D. Velic, E. Knoesel, A. Hotzel, M. Wolf, G. Ertl, *Phys. Rev. Lett.* **1998**, *80*, 2004-2007.
[20] B. E. Bent, *Chem. Rev.* **1996**, *96*, 1361-1390.
[21] a) C. Loppacher, M. Guggisberg, O. Pfeiffer, E. Meyer, M. Bammerlin, R. Lüthi, R. Schlittler, J. K. Gimzewski, H. Tang, C. Joachim, *Phys. Rev. Lett.* **2003**, *90*, 066107; b) F. Moresco, G. Meyer, K.-H. Rieder, H. Tang, A. Gourdon, C. Joachim, *Phys. Rev. Lett.* **2001**, *86*, 672-675.
[22] B. Joalland, Y. Shi, A. D. Estillore, A. Kamasah, A. M. Mebel, A. G. Suits, *J. Phys. Chem. A* **2014**, *118*, 9281-9295.
[23] A. H. Zewail, *Femtochemistry: Ultrafast Dynamics of the Chemical Bond*, World Scientific Publishing Company, **1994**
[24] J. A. Stroscio, R. M. Feenstra, *Methods in Experimental Physics,* Academic Press, **1993**, *27*, 95-147.
[25] a）S. Weigelt, C. Busse, C. Bombis, M. M. Knudsen, K. V. Gothelf, T. Strunskus, C. Wöll, M. Dahlbom, B. Hammer, E. Lægsgaard, F. Besenbacher, T. R. Linderoth, *Angew. Chem. –Int. Edit.* **2007**, *46*, 9227-9230; b）N. A. A. Zwaneveld, R. Pawlak, M. Abel, D. Catalin, D. Gigmes, D. Bertin, L. Porte, *J. Am. Chem. Soc.* **2008**, *130*, 6678-6679; c）F. Bebensee, C. Bombis, S. R. Vadapoo, J. R. Cramer, F. Besenbacher, K. V. Gothelf, T. R. Linderoth, *J. Am. Chem. Soc.* **2013**, *135*, 2136-2139.
[26] H. D. Beckey, *J. Mass Spectrom. Ion Phys.* **1969**, *2*, 500-502.
[27] R. S. Becker, J. A. Golovchenko, B. S. Swartzentruber, *Nature* **1987**, *325*, 419-421.
[28] I.-W. Lyo, P. Avouris, *Science* **1991**, *253*, 173-176.
[29] H. Uchida, D. Huang, F. Grey, M. Aono, *Phys. Rev. Lett.* **1993**, *70*, 2040-2043.
[30] P. Molinàs-Mata, A. J. Mayne, G. Dujardin, *Phys. Rev. Lett.* **1998**, *80*, 3101-3104.
[31] R. Bennewitz, J. N. Crain, A. Kirakosian, J. L. Lin, J. L. McChesney, D. Y. Petrovykh, F. J. Himpsel, *Nanotechnology* **2002**, *13*, 499-502.
[32] S. Hosoki, S. Hosaka, T. Hasegawa, *Appl. Surf. Sci.* **1992**, *60-61*, 643-647.
[33] T. Schimmel, R. Kemnitzer, J. Küppers, H. Fuchs, M. Lux-Steiner, *Thin Solid Films* **1995**, *254*, 147-152.
[34] M. Alemani, M. V. Peters, S. Hecht, K.-H. Rieder, F. Moresco, L. Grill, *J. Am. Chem. Soc.* **2006**, *128*, 14446-14447; b） M. Alemani, S. Selvanathan, F. Ample, M. V. Peters, K.-H. Rieder, F. Moresco, C. Joachim, S. Hecht, L. Grill, *J. Phys. Chem. C* **2008**, *112*, 10509-10514.
[35] C. Dri, M. V. Peters, J. Schwarz, S. Hecht, L. Grill, *Nat. Nanotechnol.* **2008**, *3*, 649-653.
[36] L. J. Whitman, J. A. Stroscio, R. A. Dragoset, R. J. Celotta, *Science* **1991**, *251*, 1206-1210.
[37] a）H. F. Ralph, L. Nordheim, *Proceedings of the Royal Society of London. Series A, Containing Papers of a Mathematical and Physical Character* **1928**, *119*, 173-181; b）V. T. Binh, N. Garcia, S. T. Purcell, *Advances in Imaging and Electron Physics,* Elsevier, **1996**, *95,* 63-153; c）K. Morgenstern, N. Lorente, K.-H. Rieder, *Physica Status Solidi (b)* **2013**, *250*, 1671-1751.
[38] a）G. Dujardin, R. E. Walkup, P. H. Avouris, *Science* **1992**, *255*, 1232; b）R. Martel, P. Avouris, I. W. Lyo, *Science* **1996**, *272*, 385-388.
[39] B. C. Stipe, M. A. Rezaei, W. Ho, *Phys. Rev. Lett.* **1997**, *79*, 4397-4400.
[40] B. C. Stipe, M. A. Rezaei, W. Ho, S. Gao, M. Persson, B. I. Lundqvist, *Phys. Rev. Lett.* **1997**, *78*, 4410-4413.
[41] a）H. Kurata, C. Colliex, *Phys. Rev. B* **1993**, *48*, 2102-2108; b）G. P. Salam, M. Persson, R. E. Palmer, *Phys. Rev. B* **1994**, *49*, 10655-10662; c）S. Gao, M. Persson, B. I. Lundqvist, *Phys. Rev. B* **1997**, *55*, 4825-4836.
[42] J. R. Hahn, W. Ho, *J. Chem. Phys.* **2005**, *122*, 244704.
[43] C. Sprodowski, M. Mehlhorn, K. Morgenstern, *J. Phys.: Condens. Matter* **2010**, *22*, 264005.
[44] a) J. K. Gimzewski, T. A. Jung, M. T. Cuberes, R. R. Schlittler, *Surf. Sci.* **1997**, *386*, 101-114. b) P. Maksymovych, D. C. Sorescu, K. D. Jordan, J. T. Yates, *Science* **2008**, *322*, 1664-1667.
[45] J. Gaudioso, H. J. Lee, W. Ho, *J. Am. Chem. Soc.* **1999**, *121*, 8479-8485.
[46] L. J. Lauhon, W. Ho, *Phys. Rev. Lett.* **2000**, *84*, 1527-1530.
[47] L. J. Lauhon, W. Ho, *J. Phys. Chem. A* **2000**, *104*, 2463-2467.
[48] J. W. Gadzuk, *Surf. Sci.* **1995**, *342*, 345-358.
[49] S.-W. Hla, G. Meyer, K.-H. Rieder, *Chem. Phys. Lett.* **2003**, *370*, 431-436.
[50] Y. Jiang, Q. Huan, L. Fabris, G. C. Bazan, W. Ho, *Nat. Chem.* **2012**, *5*, 36-41.
[51] P. Liljeroth, J. Repp, G. Meyer, *Science* **2007**, *317*, 1203-1206.
[52] A. Sperl, J. Kröger, R. Berndt, *Angew. Chem. –Int. Edit.* **2011**, *50*, 5294-5297.
[53] W. Auwärter, K. Seufert, F. Bischoff, D. Ecija, S. Vijayaraghavan, S. Joshi, F. Klappenberger, N. Samudrala, J. V. Barth, *Nat. Nanotechnol.* **2011**, *7*, 41-46.
[54] a）T. Kumagai, F. Hanke, S. Gawinkowski, J. Sharp, K. Kotsis, J. Waluk, M. Persson, L. Grill, *Phys. Rev. Lett.* **2013**, *111*, 246101; b）J. N.

Ladenthin, L. Grill, S. Gawinkowski, S. Liu, J. Waluk, T. Kumagai, *ACS Nano* **2015**, *9*, 7287-7295.
[55] T. Kumagai, F. Hanke, S. Gawinkowski, J. Sharp, K. Kotsis, J. Waluk, M. Persson, L. Grill, *Nat. Chem.* **2013**, *6*, 41-46.
[56] a）L. Gao, W. Ji, Y. B. Hu, Z. H. Cheng, Z. T. Deng, Q. Liu, N. Jiang, X. Lin, W. Guo, S. X. Du, W. A. Hofer, X. C. Xie, H. J. Gao, *Phys. Rev. Lett.* **2007**, *99*, 106402; b）E. Minamitani, N. Tsukahara, D. Matsunaka, Y. Kim, N. Takagi, M. Kawai, *Phys. Rev. Lett.* **2012**, *109*, 086602.
[57] V. Iancu, A. Deshpande, S.-W. Hla, *Nano Lett.* **2006**, *6*, 820-823.
[58] A. Zhao, Q. Li, L. Chen, H. Xiang, W. Wang, S. Pan, B. Wang, X. Xiao, J. Yang, J. G. Hou, Q. Zhu, *Science* **2005**, *309*, 1542-1544.
[59] R. Li, N. Li, H. Wang, A. Weismann, Y. Zhang, S. Hou, K. Wu, Y. Wang, *Chem. Commun.* **2018**, *54*, 9135-9138.
[60] H. Kim, Y. H. Chang, S.-H. Lee, Y.-H. Kim, S.-J. Kahng, *ACS Nano* **2013**, *7*, 9312-9317.
[61] N. Tsukahara, E. Minamitani, Y. Kim, M. Kawai, N. Takagi, *J. Chem. Phys.* **2014**, *141*, 054702.
[62] Y.-S. Fu, S.-H. Ji, X. Chen, X.-C. Ma, R. Wu, C.-C. Wang, W.-H. Duan, X.-H. Qiu, B. Sun, P. Zhang, J.-F. Jia, Q.-K. Xue, *Phys. Rev. Lett.* **2007**, *99*, 256601.
[63] H. J. Lee, W. Ho, *Science* **1999**, *286*, 1719-1722.
[64] J. Mielke, F. Hanke, M. V. Peters, S. Hecht, M. Persson, L. Grill, *J. Am. Chem. Soc.* **2015**, *137*, 1844-1849.
[65] J. Repp, G. Meyer, S. Paavilainen, F. E. Olsson, M. Persson, *Science* **2006**, *312*, 1196-1199.
[66] Y. Kim, T. Komeda, M. Kawai, *Phys. Rev. Lett.* **2002**, *89*, 126104.
[67] B. Schuler, S. Fatayer, F. Mohn, N. Moll, N. Pavliček, G. Meyer, D. Peña, L. Gross, *Nat. Chem.* **2016**, *8*, 220-224.
[68] F. Schulz, F. Garcia, K. Kaiser, D. Perez, E. Guitian, L. Gross, D. Peña, *Angew. Chem. Int. Ed*. **2019,** *58*, 9038-9042
[69] N. Pavliček, P. Gawel, D. R. Kohn, Z. Majzik, Y. Xiong, G. Meyer, H. L. Anderson, L. Gross, *Nat. Chem.* **2018**, *10*, 853-858.
[70] M. X. Yang, M. Xi, H. Yuan, B. E. Bent, P. Stevens, J. M. White, *Surf. Sci.* **1995**, *341*, 9-18.
[71] S. W. Hla, L. Bartels, G. Meyer, K.-H. Rieder, *Phys. Rev. Lett.* **2000**, *85*, 2777-2780.
[72] L. E. Dinca, J. M. MacLeod, J. Lipton-Duffin, C. Fu, D. Ma, D. F. Perepichka, F. Rosei, *Chem. Commun.* **2014**, *50*, 8791-8793.
[73] R. Gutzler, L. Cardenas, J. Lipton-Duffin, M. El Garah, L. E. Dinca, C. E. Szakacs, C. Fu, M. Gallagher, M. Vondráček, M. Rybachuk, D. F. Perepichka, F. Rosei, *Nanoscale* **2014**, *6*, 2660-2668.
[74] L. Grill, M. Dyer, L. Lafferentz, M. Persson, M. V. Peters, S. Hecht, *Nat. Nanotechnol.* **2007**, *2*, 687-691.
[75] L. Lafferentz, V. Eberhardt, C. Dri, C. Africh, G. Comelli, F. Esch, S. Hecht, L. Grill, *Nat. Chem.* **2012**, *4*, 215-220.
[76] a）M. G. Schwab, A. Narita, Y. Hernandez, T. Balandina, K. S. Mali, S. De Feyter, X. Feng, K. Müllen, *J. Am. Chem. Soc.* **2012**, *134*, 18169-18172; b） M. El Gemayel, A. Narita, L. F. Dössel, R. S. Sundaram, A. Kiersnowski, W. Pisula, M. R. Hansen, A. C. Ferrari, E. Orgiu, X. Feng, K. Müllen, P. Samorí, *Nanoscale* **2014**, *6*, 6301-6314; c）A. Narita, I. A. Verzhbitskiy, W. Frederickx, K. S. Mali, S. A. Jensen, M. R. Hansen, M. Bonn, S. De Feyter, C. Casiraghi, X. Feng, K. Müllen, *ACS Nano* **2014**, *8*, 11622-11630; d）I. Ivanov, Y. Hu, S. Osella, U. Beser, H. I. Wang, D. Beljonne, A. Narita, K. Müllen, D. Turchinovich, M. Bonn, *J. Am. Chem. Soc.* **2017**, *139*, 7982-7988; e）Y. Hu, P. Xie, M. De Corato, A. Ruini, S. Zhao, F. Meggendorfer, L. A. Straasø, L. Rondin, P. Simon, J. Li, J. J. Finley, M. R. Hansen, J.-S. Lauret, E. Molinari, X. Feng, J. V. Barth, C.-A. Palma, D. Prezzi, K. Müllen, A. Narita, *J. Am. Chem. Soc.* **2018**, *140*, 7803-7809; f）A. Narita, Z. Chen, Q. Chen, K. Müllen, *Chem. Sci.* **2019**, *10*, 964-975.
[77] L. Talirz, P. Ruffieux, R. Fasel, *Adv. Mater.* **2016**, *28*, 6222-6231.
[78] J. Cai, P. Ruffieux, R. Jaafar, M. Bieri, T. Braun, S. Blankenburg, M. Muoth, A. P. Seitsonen, M. Saleh, X. Feng, K. Müllen, R. Fasel, *Nature* **2010**, *466*, 470-473.
[79] A. Kimouche, M. M. Ervasti, R. Drost, S. Halonen, A. Harju, P. M. Joensuu, J. Sainio, P. Liljeroth, *Nat. Commun.* **2015**, *6*, 10177.
[80] H. Zhang, H. Lin, K. Sun, L. Chen, Y. Zagranyarski, N. Aghdassi, S. Duhm, Q. Li, D. Zhong, Y. Li, K. Müllen, H. Fuchs, L. Chi, *J. Am. Chem. Soc.* **2015**, *137*, 4022-4025.
[81] A. Basagni, F. Sedona, C. A. Pignedoli, M. Cattelan, L. Nicolas, M. Casarin, M. Sambi, *J. Am. Chem. Soc.* **2015**, *137*, 1802-1808.
[82] Y.-C. Chen, D. G. de Oteyza, Z. Pedramrazi, C. Chen, F. R. Fischer, M. F. Crommie, *ACS Nano* **2013**, *7*, 6123-6128.
[83] a）K. Nakada, M. Fujita, G. Dresselhaus, M. S. Dresselhaus, *Phys. Rev. B* **1996**, *54*, 17954-17961; b）L. Yang, C.-H. Park, Y.-W. Son, M. L. Cohen, S. G. Louie, *Phys. Rev. Lett.* **2007**, *99*, 186801.
[84] P. Ruffieux, S. Wang, B. Yang, C. Sánchez-Sánchez, J. Liu, T. Dienel, L. Talirz, P. Shinde, C. A. Pignedoli, D. Passerone, T. Dumslaff, X. Feng, K. Müllen, R. Fasel, *Nature* **2016**, *531*, 489-492.
[85] a）S. Linden, D. Zhong, A. Timmer, N. Aghdassi, J. H. Franke, H. Zhang, X. Feng, K. Müllen, H. Fuchs, L. Chi, H. Zacharias, *Phys. Rev. Lett.* **2012**, *108*, 216801; b）J. D. Teeter, P. S. Costa, M. Mehdi Pour, D. P. Miller, E. Zurek, A. Enders, A. Sinitskii, *Chem. Commun.* **2017**, *53*, 8463-8466.
[86] a）D. G. de Oteyza, A. García-Lekue, M. Vilas-Varela, N. Merino-Díez, E. Carbonell-Sanromá, M. Corso, G. Vasseur, C. Rogero, E. Guitián, J. I. Pascual, J. E. Ortega, Y. Wakayama, D. Peña, *ACS Nano* **2016**, *10*, 9000-9008; b）C. Sánchez-Sánchez, T. Dienel, O. Deniz, P. Ruffieux, R. Berger, X. Feng, K. Müllen, R. Fasel, *ACS Nano* **2016**, *10*, 8006-8011.
[87] H. Sakaguchi, S. Song, T. Kojima, T. Nakae, *Nat. Chem.* **2016**, *9*, 57-63.
[88] D. Beyer, S. Wang, C. A. Pignedoli, J. Melidonie, B. Yuan, C. Li, J. Wilhelm, P. Ruffieux, R. Berger, K. Müllen, R. Fasel, X. Feng, *J. Am. Chem. Soc.* **2019**, *141*, 2843-2846.
[89] J. Cai, C. A. Pignedoli, L. Talirz, P. Ruffieux, H. Söde, L. Liang, V. Meunier, R. Berger, R. Li, X. Feng, K. Müllen, R. Fasel, *Nat. Nanotechnol.* **2014**, *9*, 896-900.
[90] R. R. Cloke, T. Marangoni, G. D. Nguyen, T. Joshi, D. J. Rizzo, C. Bronner, T. Cao, S. G. Louie, M. F. Crommie, F. R. Fischer, *J. Am. Chem. Soc.* **2015**, *137*, 8872-8875.
[91] a）Y.-F. Zhang, Y. Zhang, G. Li, J. Lu, Y. Que, H. Chen, R. Berger, X. Feng, K. Müllen, X. Lin, Y.-Y. Zhang, S. Du, S. T. Pantelides, H.-J. Gao, *Nano Res.* **2017**, *10*, 3377-3384; b）R. A. Durr, D. Haberer, Y.-L. Lee, R. Blackwell, A. M. Kalayjian, T. Marangoni, J. Ihm, S. G. Louie, F. R. Fischer, *J. Am. Chem. Soc.* **2018**, *140*, 807-813.
[92] X.-Y. Wang, J. I. Urgel, G. B. Barin, K. Eimre, M. Di Giovannantonio, A. Milani, M. Tommasini, C. A. Pignedoli, P. Ruffieux, X. Feng, R. Fasel, K. Müllen, A. Narita, *J. Am. Chem. Soc.* **2018**, *140*, 9104-9107.
[93] C. Ma, Z. Xiao, J. Huang, L. Liang, W. Lu, K. Hong, B. G. Sumpter, J. Bernholc, A.-P. Li, *Phys. Rev. Mater.* **2019**, *3*, 016001.
[94] Y. Okawa, M. Aono, *Nature* **2001**, *409*, 683-684.
[95] Y. Okawa, M. Akai-Kasaya, Y. Kuwahara, S. K. Mandal, M. Aono, *Nanoscale* **2012**, *4*, 3013-3028.
[96] a) Y. Okawa, M. Aono, *J. Chem. Phys.* **2001**, *115,* 2317-2322; b）A. Miura, S. De Feyter, M. M. S. Abdel-Mottaleb, A. Gesquière, P. C. M. Grim, G. Moessner, M. Sieffert, M. Klapper, K. Müllen, F. C. De Schryver, *Langmuir* **2003**, *19*, 6474-6482; c）Y. Yang, M. B. Zimmt, *Langmuir* **2015**, *31*, 12408-12416.
[97] L. Verstraete, B. E. Hirsch, J. Greenwood, S. De Feyter, *Chem. Commun.* **2017**, *53*, 4207-4210.
[98] S. Clair, O. Ourdjini, M. Abel, L. Porte, *Chem. Commun.* **2011**, *47*, 8028-8030.
[99] Y. B. Zhao, D. M. Poirier, R. J. Pechman, J. H. Weaver, *Appl. Phys. Lett.* **1994**, *64*, 577-579.
[100] Y. Nakamura, F. Kagawa, K. Kasai, Y. Mera, K. Maeda, *Surf. Sci.* **2003**, *528*, 151-155.
[101] a）Y. Nakamura, Y. Mera, K. Maeda, *Appl. Phys. Lett.* **2000**, *77*, 2834-2836; b）Y. Nakamura, F. Kagawa, K. Kasai, Y. Mera, K. Maeda, *Appl. Phys. Lett.* **2004**, *85*, 5242-5244; c）Y. Nakamura, Y. Mera, K. Maeda, *Jpn. J. Appl. Phys.* **2005**, *44*, L1373-L1376.

[102] M. Nakaya, S. Tsukamoto, Y. Kuwahara, M. Aono, T. Nakayama, *Adv. Mater.* **2010**, *22*, 1622-1625.
[103] R. Meir, H. Chen, W. Lai, S. Shaik, *ChemPhysChem* **2010**, *11*, 301-310.
[104] A. C. Aragonès, N. L. Haworth, N. Darwish, S. Ciampi, N. J. Bloomfield, G. G. Wallace, I. Diez-Perez, M. L. Coote, *Nature* **2016**, *531*, 88-91.
[105] a）Y. Okawa, S. K. Mandal, C. Hu, Y. Tateyama, S. Goedecker, S. Tsukamoto, T. Hasegawa, J. K. Gimzewski, M. Aono, *J. Am. Chem. Soc.* **2011**, *133*, 8227-8233; b） M. Nakaya, Y. Okawa, C. Joachim, M. Aono, T. Nakayama, *ACS Nano* **2014**, *8*, 12259-12264.
[106] a）M.-S. Liao, S. Scheiner, *J. Chem. Phys.* **2001**, *114*, 9780-9791; b） H. Shinohara, O. Tsaryova, G. Schnurpfeil, D. Wöhrle, *J. Photochem. Photobiol. A* **2006**, *184*, 50-57.
[107] a) L. Gross, F. Mohn, N. Moll, P. Liljeroth, G. Meyer, Science 2009, 325, 1110-1114; b) Y. Sugimoto, M. Abe, S. Hirayama, N. Oyabu, Ó. Custance, S. Morita, *Nat. Mater.* **2005**, *4*, 156-159; c）Y. Sugimoto, P. Pou, O. Custance, P. Jelinek, M. Abe, R. Perez, S. Morita, *Science* **2008**, *322*, 413-417; d）J. N. Ladenthin, T. Frederiksen, M. Persson, J. C. Sharp, S. Gawinkowski, J. Waluk, T. Kumagai, *Nat. Chem.* **2016**, *8*, 935-940.
[108] N. Pavliček, A. Mistry, Z. Majzik, N. Moll, G. Meyer, D. J. Fox, L. Gross, *Nat. Nanotechnol.* **2017**, *12*, 308-311.